ATTENUATED TOTAL REFLECTANCE FOURIER TRANSFORM INFRARED SPECTROSCOPY OF FLUID SYSTEMS: CASE STUDY APPLICATIONS TO DIAGNOSIS AND SCREENING IN BIOMEDICAL AND FOOD AREAS

A THESIS SUBMITTED TO
THE GRADUATE SCHOOL OF NATURAL AND APPLIED SCIENCES
OF
MIDDLE EAST TECHNICAL UNIVERSITY

BY

SEHER GÖK

IN PARTIAL FULFILLMENT OF THE REQUIREMENTS
FOR
THE DEGREE OF MASTER OF SCIENCE

IN

BIOLOGY

AUGUST 2013

Approval of the Thesis

ATTENUATED TOTAL REFLECTANCE FOURIER TRANSFORM INFRARED SPECTROSCOPY OF FLUID SYSTEMS: CASE STUDY APPLICATIONS TO DIAGNOSIS AND SCREENING IN BIOMEDICAL AND FOOD AREAS

submitted by **SEHER GÖK** in partial fulfillment of the requirements for the degree of **Master of Science in Biology Department, Middle East Technical University** by,

Prof. Dr. Canan Özgen _____
Dean, Graduate School of **Natural and Applied Sciences**

Prof. Dr. Gülay Özcengiz _____
Head of Department, **Biology**

Prof. Dr. Feride Severcan _____
Supervisor, **Biological Sciences Dept., METU**

Examining Committee Members:

Assoc. Prof. Dr. Sertaç Önde _____
Biological Sciences Dept., METU

Prof. Dr. Feride Severcan _____
Biological Sciences Dept., METU

Assoc. Prof. Dr. Hakan Altan _____
Department of Physics, METU

Assist. Prof. Dr. Şebnem Garip _____
Faculty of Medicine, Istanbul Kemerburgaz Unv.

Assist. Prof. Dr. Yekbun Adıgüzel _____
Faculty of Medicine, Istanbul Kemerburgaz Unv.

Date: _____

I hereby declare that all information in this document has been obtained and presented in accordance with academic rules and ethical conduct. I also declare that, as required by these rules and conduct, I have fully cited and referenced all material and results that are not original to this work.

Name, Last name: Seher, Gök

Signature :

ABSTRACT

ATTENUATED TOTAL REFLECTANCE FOURIER TRANSFORM INFRARED SPECTROSCOPY OF FLUID SYSTEMS: CASE STUDY APPLICATIONS TO DIAGNOSIS AND SCREENING IN BIOMEDICAL AND FOOD AREAS

Gök, Seher
M.Sc., Department of Biology
Supervisor: Prof. Dr. Feride Severcan

August 2013, 85 pages

ATR-FTIR spectroscopy offers highly specific, sensitive, label free and non-destructive analytical examination opportunity for biological systems. Despite the many progresses in order to improve biological applications of this powerful technique, there has not yet been acquired enough end user data that were exemplified by proper case studies. Here, two case studies, from biomedical and food areas were retrieved to illustrate the influential potential of ATR-FTIR technique for diagnosis and screening of biological systems.

In the first case study, ATR-FTIR spectroscopy was used for the investigation of bladder tumor presence, using bladder wash sample. Current gold standard diagnosis techniques have some inadequacies. Macromolecular investigations on the ATR-FTIR spectra showed up many carcinogenesis induced differences between control and carcinoma groups. Conspicious increase in nucleic acid and protein content was revealed in carcinoma group in addition to the structural changes in carbohydrate and proteins. Discrimination sensitivity and specificity in the 1100-900 cm^{-1} spectral region, with the values of 92.5% and 68% respectively, were achieved by hierarchical clustering of control and carcinoma samples. Attained results demonstrated that, ATR-FTIR can be used for bladder tumor detection from bladder wash sample with higher overall sensitivity than urine cytology.

In the second case study, ATR-FTIR spectroscopy was coupled with multivariate analysis including Principal Component and Hierarchical Clustering analysis for the classification of Turkey honey samples based on their botanical origin. For botanical origin estimations, new analytical techniques have been looked for as an alternative to labor intensive and

less sensitive classical techniques. It is the first time that the Turkish honey samples have been investigated experimentally for botanical origin estimation with ATR-FTIR. Discrimination was achieved with 100% sensitivity and specificity over the spectral range of 1800-750 cm^{-1} with cluster analysis. PCA results also in consisted with the hierarchical clustering analysis results.

Keywords: ATR-FTIR, bladder wash, honey botanical origin, cluster, PCA

ÖZ

SIVI SİSTEMLERDE AZALTILMIŞ TOPLAM YANSIMALI FOURİER DÖNÜŞÜMLÜ KIZILÖTESİ SPEKTROSKOPİSİ: BİYOMEDİKAL VE GIDA ALANLARINDA TANI VE TARAMADA UYGULAMA ÖRNEKLERİ

Gök, Seher
Yüksek Lisans, Biyoloji Bölümü
Tez Yöneticisi: Prof. Dr. Feride Severcan

Ağustos 2013, 85 sayfa

ATR-FTIR spektroskopisi, biyolojik sistemlerde, oldukça hassas, özgül, tahribatsız ve herhangi bir işaretleyici molekülden bağımsız olarak analitik inceleme olanağı tanıyan bir yöntem olarak karşımıza çıkmaktadır. Bu güçlü tekniğin biyolojik uygulamalarını geliştirmek amacıyla oldukça yol kat edilmesine rağmen henüz yeteri kadar örnek çalışmalarla tasdik edilmiş son kullanıcı verileri bulunmamaktadır. Bu çalışmada, biyomedikal ve gıda alanlarından iki örnek çalışma verilerek ATR-FTIR tekniğinin biyolojik sistemlerin tanı ve taramasında etkin kullanılabilirlik potansiyeli gösterilmiştir.

İlk çalışmada, ATR-FTIR spektroskopisi mesane yıkama sıvısından mesane tümörü varlığının araştırılması amacıyla kullanılmıştır. Hali hazırda kullanılan ve altın standart olarak kabul edilen teşhis yöntemlerinin bazı eksiklikleri bulunmaktadır. ATR-FTIR spektrumları üzerinde yapılan makromoleküler incelemelerle, kontrol ve karsinoma grupları arasında kanser oluşumuna bağlı değişikler gösterilmiştir. Karsinoma grubunda nükleik asit ve protein miktarındaki kayda değer bir yükselmenin yanı sıra karbonhidrat ve proteinlerin yapısal değişiklikleri açığa çıkarılmıştır. 1100-900 cm^{-1} spektral bant aralığında, kontrol ve karsinoma gruplarının ayrımı %92,5 hassalık ve %68 duyarlılıkla elde edilmiştir. Elde edilen sonuçlar, ATR-FTIR spektroskopisinin, mesane yıkama sıvısından mesane tümörü teşhisinde, idrar sitolojisinden daha yüksek duyarlılıkla kullanılabilir olduğunu göstermiştir.

İkinci çalışmada, ATR-FTIR spektroskopisi çok değişkenli analiz yöntemlerinden birincil bileşen ve hiyerarşik kümeleme analizleri ile birlikte, Türk ballarının botanik kökenlerine göre sınıflandırılması amacıyla kullanılmıştır. Botanik köken tahmini için, zahmetli ve

hassaslığı düşük klasik tekniklere alternatif olabilecek yeni analitik teknikler araştırılmaktadır.

Bu çalışmada ilk kez Türk balları ATR-FTIR spektroskopisi kullanılarak botanik köken tesbiti amacıyla deneysel olarak incelenmektedir. 1800-750 cm^{-1} spektral bant aralığında, %100 hassaslık ve duyarlılıkta tüm incelenen bal gruplarının ayrımı elde edilmiştir. PCA sonuçları da hiyerarşik kümeleme analizi sonuçlarını destekler mahiyettedir.

Anahtar kelimeler: ATR-FTIR, mesane yıkama sıvısı, bal botanik köken, kümeleme, PCA

To My Family,

ACKNOWLEDGEMENTS

I would like to thank to my supervisor Prof. Dr. Feride SEVERCAN for her guidance, patience, encouragement and supervision throughout this thesis study. I am also deeply indebted to Dr.Ferruh Zorlu with whom we carried out the first part of the project. He was very helpful during the project and their innovative ideas impressed me a lot.

I also compassionately express my special thanks to Nihal Ozek and Seza Ergun owing to their precious help and lovely attitude in the course of experimental period and writing this thesis. I would like to thank also to everyone in the biophysics group who were always there when I needed help and who gave me the possibility for having a very good time during this study. I would like to extend my thanks to my beloved homemate Duygu Varol for her patience, support and friendship.

I would like to send my ultimate appreciation to my parents for their endless patience, encouragement, support and love.

TABLE OF CONTENTS

LIST OF TABLES

TABLES

LIST OF FIGURES

FIGURES

CHAPTER I

INTRODUCTION

Within this chapter, primarily general information about the bladder cancer and bladder tumor detection techniques was given briefly. The usage of FTIR spectroscopy in cancer detection in the literature was also summarized. In the second part brief review about the botanical origin determination of honey was presented. In the last part, the basis and applications of biophysical technique, ATR-FTIR spectroscopy, which had been used throughout this study, were explained.

Part I : Bladder Cancer

1.1 Bladder Anatomy

Urinary bladder is the hollow, muscular organ which reserves urine, collected from the kidneys through the ureters, before disposal by urination through the urethra. It is positioned in the lower pelvic cavity. Specifically; in men, it sits on the anterior to the rectum and in women, it situates anterior to the vagina.

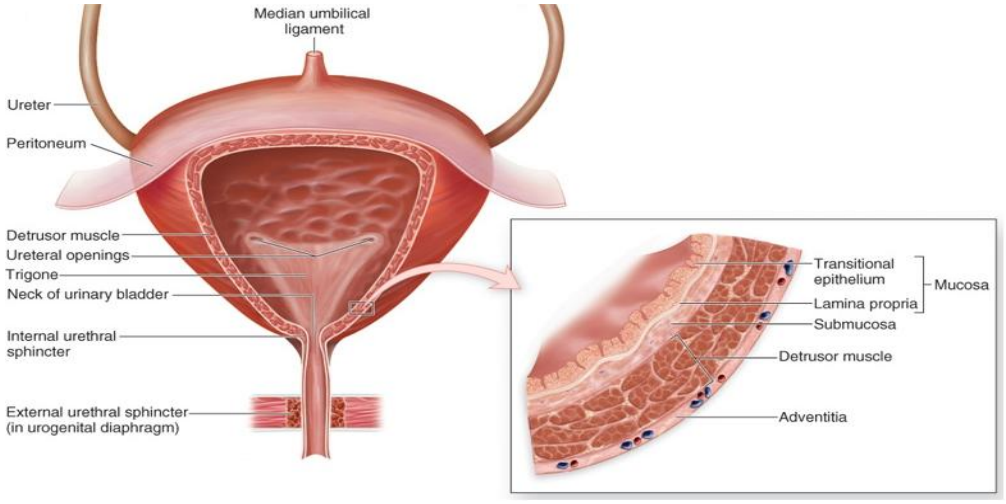

Figure 1-1 Schematic diagram of urinary bladder (Adopted from The McGraw Companies, Inc.)

Bladder wall composed of submucosa; lamina propria, muscularis, perivesical fat and serosa layers from inner side to the outer. 4 – 8 layers of transitional epithelial cells (urethelium) which are able to change shape from cuboidal cells to squamous cells, form the mucosa layer. Epithelial cells are seperated from the connective tissue by a basement membrane. Lamina propria, epithelium beneath the connective tissue, contains elastic and collagen fibers, nerves and blood vessels. Loosely arranged smooth muscle and elastic fibers made up of the muscularis. Contraction of this muscle layer controls the urination. The outermost layer, serosa, is visceral peritoneum which covers the upper region of urinary bladder. Serosa composed of collagen and elastic fibers, neurons, neuronal ganglions and blood vessels (Campbell-Walsh Urology, 2007).

1.2 Epidemiology of Bladder Cancer

Bladder cancer is a malignant neoplasm, originates from the epithelial cells of the bladder, and one of the most common urogenital cancer in the world. Although bladder tumor is observed in all age groups, it is an advanced age disease. The mean incidence age is 69 in men and 71 in women. According to the statistics, bladder cancer stated as the seventh most common cause of deaths among USA and UK males. The incidence of bladder cancer increases directly proportionally with the increasing age. It was estimated that, 386,300 new cases and 150,200 deaths had occurred in 2008 worldwide. In overall cancer frequencies it was ranked as 6^{th}. Bladder cancer incidence show significant difference by sex; male to female ratio was given as 3.8 : 1 (Jemal et al., 2011).

In Turkey, according to the study report depending on the 8 provinces cancer database, standardized incidence rate was estimated as 19.6/100000 and 2.5/100000 in man and woman respectively, in 2006. It was stated as the 3^{rd} most commonly seen cancer in men and 13^{th} in women. The most common incidence rates were observed in İzmir & Eskişehir for men and in Antalya & Eskişehir for women (Eser et al., 2006).

1.3 Etiology of Bladder Cancer

Bladder cancer development is multi-factorial. It was reported that, occupational exposure to chemicals, smoking, parasitic, bacterial and viral infections, the presence of urinary tract diseases, consumption of analgesics, genotoxic and chemotherapeutic agents, some specific polymorphisms, chromosomal anomalies and genomic aberrations could be associated with the development and progression of bladder cancer.

Smoking can be stated as the most prominent risk factor, as it increases the risk 4 times in cigarette smokers. Risk rises proportionally with the cigarette consumption amount, inhalation degree, and exposure year (Castelao et al., 2001).

Aromatic amines like 4-aminobiphenyl, are main carcinogens in tobacco smoke. Aromatic amines constitute a risk for bladder cancer by generating the reactive electrophiles, DNA adduct formations and mutations as they are metabolically N-hydroxylated and esterified compounds (Jiang et al., 2007).

It was shown that smoking promote the proliferative response of bladder epithelial via activating the Stat3/ERK1/2 and leading to the induction of Stat3 and NF-κB DNA binding activity which results in cyclin D1 expression thus enhances the cell proliferation (Chen et al., 2008) and increases the effects of other carcinogens and genetic predisposition (Ouerhani et al., 2009).

The aniline dyes which have been used since the late 1800s, are urethelial carcinogens. Also, exposure to some chemicals like 2- naphthylamine, 4-aminobiphenyl, 4-nitrobiphenyl, 4-4 diaminobiphenyl; inflammable gases ; coal dust and some aldehydes like acrolein that are used is chemical dyes, rubber and textile industry are found to be associated with urethelial cancers (Steinbeck et al., 1990).

Bladder stone or catheter existence dependent chronic cystitis increases the squamous cell carcinoma risk. Schistosoma haematobium infection show direct correlation with bladder tumor progression. Chronic irritation of urethelium depending on the bacterial infection has been shown as the effective mechanism for carcinoma development (International Agency for Research on Cancer, 1994).

Also it was shown that human papilloma virus (HPV) infection plays role in bladder tumor progression in immune suppressed patients (Griffiths and Mellon, 2000).

It has been known that radiotherapy plays role in cancer development. Woman patients, who had undergone radiotherapy for pelvic malignancies, developed 2-4 times more bladder tumor (Campbell-Walsh Urology, 2007).

In addition to these, there are many other environmental factors that may contribute to the development of bladder cancer including, dietary factors, analgesic drugs, artificial sweeteners, chemotherapeutic agents, race, gender and socioeconomic status.

Genetic susceptibility also play important role in urethelial bladder cancer development. Risk is 2 folds higher in first degree relatives of bladder cancer patients. Slow acylator N-acetyltransferase 2 (NAT2) variants and glutathione S-transferase mu 1 (GSTM1) – null genotypes show associations in bladder cancer cases (Wu et al., 2009). NAT2 enzymes contribute to detoxification of some carcinogens so a slow NAT2 acylator genotype was encountered to be a genetic risk factor especially in smoker patients (Gu et al., 2005).

Although studies have not shed light on complete genetic mechanisms, it has been thought more than one genetic mechanisms affect the development of bladder cancer.

The activation of oncogenes and the loss of function of tumor suppressor genes are main reasons for tumor growth. The loss of genetic material on the q arm of 9^{th} chromosome (9q) is constantly detected as a symptom in both low and high grade and stage bladder cancer cases. Also in the 40% of bladder cancer cases, deletion of 11p including the c-Ha-ras proto-oncogene, was observed. In the 60% of cases deletions on chromosome 17p was observed. As p53 tumor suppressor gene localizes on 17p, findings are evaluated as significant (Campbell-Walsh Urology, 2007).

1.4 Pathology of Bladder Cancer

90% of the bladder tumors are transitional (Urethelial) cell carcinomas (TCC). While the 70-85% of them is superficial tumors, 10-20% of them progress the muscle invasive disease. The remaining 10% of the bladder malignant neoplasm are composed of squamous cell carcinomas and adenocarcinomas (Campbell-Walsh Urology, 2007).

1.4.1 Epithelial Hyperplasia and Metaplasia

Epithelial hyperplasia indicates the increase in number without nuclear and structural anomalies in cells.

Urethelial metaplasia has nontransitioanl epithelial appearance with squamous or glandular metaplasia development in focal areas in bladder wall. They are indicated as benign cases (Campbell-Walsh Urology, 2007).

1.4.2 Dysplasia

Dysplasia is an intermediate epithelial alteration between normal urethelium and carcinoma in situ (CIS).

1.4.3 Inverted papilloma

Inverted papilloma is a benign proliferative lesion mainly developed in conjunction with the chronic inflammation or obstruction on bladder. Conversion of inverted papillomas into the malign cases is rare however they are frequently seen with transitional cell carcinoma (Campbell-Walsh Urology, 2007).

1.4.4 Vesicular leucoplasia

Leocoplasia is a kind of metaplasia characterized with ceratinization, akanthosis and dysplasia. Generally this pre-malign lesion progresses to squamous cell carcinoma in 20% of patients (Campbell-Walsh Urology, 2007).

1.4.5 Urethelial Neoplasms

Transitional cell carcinoma (TCC): These cancers are histopathologically characterized as; increase in the number of epithelial layer, loss of cell polarity, abnormal cell maturation from basal layers to the surface, giant cells, nuclear congestion, increased nucleus/cytoplasm ratio and increase in chromatin structure. Transitional cell carcinomas

can be found in papillary, nodular, mixed or carcinoma in situ. 70% of cases are papillary tumors. TCC is frequently seen in trigone and bladder base (Campbell-Walsh Urology, 2007).

Carcinoma in situ (CIS): a kind of intraepithelial, superficial, anaplastic transitional cell carcinoma. As the tumor cells are loosely attached, urine cytology gives positive results in the 80-90% of cases. CIS accepted as the starting lesion of invasive bladder cancer. While CIS cases, which are seen more frequently in multiple tumors, have 20% relapse rate, they might progress into high grade muscle invasive cancer with 75% probability (Campbell-Walsh Urology, 2007).

1.4.6 Non-urethelial neoplasms

Squamous cell carcinoma: squamous cell carcinomas are generally originated depending on urinary stones, long term catheter usage or pathological chronic bladder infection. As the disease is in advanced stage mainly, in the time of diagnosis, they have bad prognosis rate. Also, there is another type of squamous cell carcinoma which develops as a result of schistoma haematobium infection. This type is observed with 75% frequency in Egypt while other version constituting the 1-7% of the squamous cell carcinomas (Campbell-Walsh Urology, 2007).

Adenocarcinoma: adenocarcinomas are categorized in 3 groups, as primer, metastatic and urachal adenocarcinomas. Chronic inflammation and irritation are showed as the primer reasons for adenocarcinomas. They are poorly differentiated invasive tumors. As they are in advanced stage in the time of prognosis, they have worse prognosis (Campbell-Walsh Urology, 2007).

Other rarely seen epithelial bladder carcinomas are villous adenomas, melanomas, carcino-sarcomas and carcinoid tumors. On the other hand, lipomas, choriocarsinomas, pheochromositomas and mesenchemial tumors are stated as the rarely seen non-epithelial tumors (Campbell-Walsh Urology, 2007).

1.5 Progression and Dissemination of Bladder Tumor

As the bladder tumor relapses are mainly seen in the old resection areas, monoclonal cell theory come into prominence related with the bladder tumor progression. Theory claims that the bladder tumor progresses from single cell and then this cell inseminates the different regions of bladder.
Mainly bladder tumors disseminate by direct invasion. Tumor on bladder mucosa progresses through basal membrane, lamina propria, muscle tissue and then outside of the

bladder consecutively. Tumors which invade the lamina propria can metastasize to regional lymph nodes and distant organs, as they come into contact with lymph and venous vessels.

In U.S. newly diagnosed bladder tumors are 55-60% well or moderately differentiated superficial and papillary transitional cell carcinomas (Messing et al., 1995).
After endoscopic resection, relapse is observed predominantly. 16-25% of these relapses are high grade tumors (Prout et al., 1992). In the 10% of the superficial papillary bladder tumors, invasion or metastasis was observed (Amling, 2001).

40-45% of the newly diagnosed bladder tumors are high grade tumors and the half of them have already been invaded to muscle.

1.5.1 Staging of the Bladder Tumors

Tumor grade and stage show significant correlation with patient survival, disease progression and recurrence rates (Soloway et al., 2003). While tumor grading is relying on the cytological characteristics, tumor stage indicates the degree of metastasis and invasiveness. Tumor stage is the most important indicator for accurate prognosis.

Not only pathological but also the clinical information is utilized for tumor staging. For staging of the bladder tumor, required tissue is gathered by transurethral tumor resection (TUR). Bimanual examination before and after TUR, doesn't give information related with the invasion of tumor on bladder wall, but when the tumor is palpable, physician could understand if the tumor invaded to muscle or not. In routine clinical trials, tumor-node- metastasis (TNM) system was developed by the collective study of International union against cancer (UICC) and American Joint Commission on cancer (AJCC), for tumor staging. Here; T indicates the invasion of primer tumor, N indicates the metastasis degree in regional lymph nodes and M indicates the degree of distant tissue and organ metastasis. Table 1-1 and Table 1-2 summarize the TNM categories.

Table 1-1 TNM Classification of Bladder Cancer

Primary Tumor (T) Stage		**Regional Lymph Nodes (N)**		**Distant Metastasis (M)**	
TX	Primary tumor cannot be assessed	NX	Regional lymph nodes cannot be assessed	MX	Distant metastasis cannot be assessed
T0	No evidence of primary tumor				
Ta	Non-invasive papillary carcinoma	N0	No regional lymph node metastasis	M0	No distant metastasis
Tis	Carcinoma in situ				
T1	Tumor invades sub epithelial connective tissue	N1	Metastasis 2cm or less	M1	Distant metastasis
T2	Tumor invades muscle				
T2a	Tumor invades superficial muscle				
T2b	Tumor invades deep muscle	N2	Metastasis more than 2 cm but not more than 5 cm		
T3	Tumor invades perivesical tissue				
T3a	Microscopic invasion of perivesical tissue				
T3b	Macroscopic invasion of perivesical tissue	N3	Metastasis more than 5 cm		
T4	Tumor invades prostate uterus, vagina, pelvic wall, abdominal wall				
T4a	Tumor invades prostate, uterus, vagina				
T4b	Tumor invades pelvic or abdominal wall				

Table 1-2 Grouping for Bladder Cancer (Greene et al., 2002)

Stage	Primary tumor classification	Regional lymph node classification	Distant metastasis classification
Stage 0a	Ta	N0	M0
Stage 0is	Tis	N0	M0
Stage I	T1	N0	M0
Stage II	T2a	N0	M0
	T2b		
Stage III	T3a	N0	
	T3b		M0
Stage IV	T4a	N0	M0
	T4b		
	Any T	N1	M0
	Any T	N2	M0
	Any T	N3	M0
	Any T	Any N	M1

1.5.2 Grading of Bladder Tumors

There is no single grading system on which the consensus is settled on. Generally grading systems based on the anaplasia degree of the tumor cells. One of the widely accepted and used grading systems was the world health organization (WHO) 1973 system where the Carcinomas are classified as papillomas, TCC grade 1 well differentiated, TCC grade 2 moderately differentiated and TCC grade 3 poorly differentiated cancers. In 1998, WHO and International Society of Urological Pathologists (ISUP) published a newly developed better classification system (Epstein et al., 1998; Reuter et al., 1999).

But this new system was not accepted by many urologists. To solve the confusion, WHO presented two new classifications in 2001 and 2004 (Table 1-3).

Table 1-3 Bladder Cancer Grading systems

WHO 1973	WHO/ISUP 1998	WHO 2001	WHO 2004
Papilloma	Papilloma	Papilloma	Papilloma
TCC Grade 1	PUNLMP	PUNLMP	PUNLMP
	TCC-Low Grade	TCC Grade 1	TCC- Low Grade
TCC Grade 2			
TCC Grade 3	TCC- High Grade	TCC Grade 2	TCC- High Grade
		TCC Grade 3	

It can be said that, for the determination of tumor aggressiveness, cytological grading is more important than histological pattern recognition (DeMay, 1995).

Lower grade tumors are kind of flat lesions. In grade 1 cancers, which are also classified as papillary urethelial neoplasms of low malignant potential (PUNLMP), urothelium might show normal maturation, cohesiveness and polarity. Additionally the mitotic signs are seen rarely but urotheliom thickened.

However, in grade 2 cancers, which are classified as low or high grade papillary urethelial carcinomas, the mitotic signs are identifiable. Also cells show atypia like; cell crowding, nuclear enlargement and hyperchromasia. Depending on the cases history, high nuclear to cytoplasmic ratio, non-vacuolated cytoplasm and irregular nuclear membranes are stated as the key features for the diagnosis of low-grade cancers (DeMay, 1995; Raab et al., 1994).

Grade 3 cancers are the most aggressive bladder cancers which generally end up with deaths. Cells show high atypia and pleomorphism. Also they have bizarre looking. Chromatin structure is altered, nucleus/cytoplasm ratio and mitotic activity is really high. In grade 3 tumors, squamous and glandular differentiations might be observed (DeMay, 1995).

1.6 Clinical Symptoms in Bladder Cancer and Diagnosis

Common presentation of bladder cancer is the macroscopic or microscopic haematuria. Muscle invasive tumor or CIS patients also come with irritative bladder symptoms like disuria, urgent and frequent urination need (Edwards et al., 2006).

1.6.1 Diagnosis

1.6.1.1 Morphology-based test

Morphology-based assays depend on the microscopical investigation of tumor cells in urine or bladder wash samples. These kind of assays are observer dependent thus highly subjective. The expertise of pathologist is so important. Also the shedding of tumor cells into the collected sample changes depending on the tumor classes and patients history, so accuracy of the interpretations varies.

Cytology: Commonly, cytology is used with cystoscopy. Assay depends on the fact that, as the adhesion is weak between malign cells; they easily flow into the voided urine or bladder wash. Malignant cells can be detected in urine long before the visible lesions become apparent in cystoscopical examination so urine cytology can be highly predictive especially in TCC cases. In low grade cancers the sensitivity of the test is not sufficient as the malignant cells and normal urotheium cells still resemble to each other. The overall sensitivity of the test varies between 40-60% (Grossman, 1998; Ramakumar et al., 1999). However in high grade T1 or Ta tumors and carcinoma in situ cases the sensitivity rises up to 90% while specificity approaches to 98-100% (Brown, 2000).

ImmunoCyt: The presence of tumor cells is investigated after staining of cells with three different tumor-specific antibodies. Assay's sensitivity is poor in low-grade and superficial tumors like in cytology (Vriesema et al., 2001).
ImmunoCyt's diagnostic potential showed less specificity than cytology and also its sensitivity varies sharply between different studies (Hautmann et al., 2004; Pfister et al., 2003).

1.6.1.2 Protein-based tests

Protein based assays principally depend on the detection of the presence or activity of cancer related proteins in urine or urinary cells. Urine, without any need for sediment preparation, can be used directly. The sensitivity of the assay associated with the grade of cancer can be based on, standard discriminative threshold level for the protein that varies between different labs, and the presence of proteinases in urine. Currently used protein-based tests are, NMP22, BTA, BTA-Stat and BTA-Trak.

1.7 FTIR Spectroscopy and Cancer

Applications of vibrational spectroscopy; especially infrared and Raman spectroscopy, is gaining great importance nowadays. Specifically the applications of spectroscopy on

biological samples notably in the detection of cancer and malignancy detection have increased great deal all over the world. Numerous biological materials including bone, skin, lung, cervix, ovary etc. have been examined with these methods. Cervical and ovarian cancer had been studied with FTIR spectroscopy. Wood et al. reported in their study that, dysplastic or malignant transformations in epithelial tissues exhibit pronounced symmetric and asymmetric phosphate modes and also the reduction in glycogen intensity. Their study revealed the potential of FTIR spectroscopy as a diagnostic cervical screening tool (Wood et al., 1996). Another FTIR microspectroscopic (FTIRM) study of the same group, aimed to investigation of variables that may be useful for cervical cancer diagnosis. They showed the malignancy dependent spectral changes in the 1300-900 cm^{-1} phosphodiester region in lymphocytes and leucocytes. Also the reduction in glycogen band area and a pronounced $v_sPO_2^-$ band in endocervical mucin were reported. R. Sindhuphak et al. compared the FTIR spectroscopy results with the histological diagnosis of cervical samples and have reached 96.3% sensitivity and 96.4% specificity (Sindhuphak et al. 2003). Fung et al. reported the differentiation of grade I and grade II adenocarcinoma from the normal human endometrium. Malignancy drived changes were observed in the CH stretching region, C-O stretching of carbohydrates and cellular proteins and the symmetric and asymmetric stretching of phosphodiester bonds in nucleic acid region (Fung et al., 1996).

Lung cancer is also widely investigated cancer type with vibrational spectroscopy. Wang et al. used pleural fluid with FTIR microspectroscopy with the aim of gathering quick results. Results indicated considerable differences between lung cancerous, normal and tuberculous cells, in the ratio of bands originated from glycogen and nucleic acids (Wang et al., 1997).

In another study, cancerous and non-cancerous human lung tissues were examined directly under FTIR microscopy for investigating the potentials of this technique in clinical diagnosis. Ratio of glycogen and cholesterol peak heights at 1045 cm^{-1} and 1465 cm^{-1} respectively, were chosen as an indicator for lung malignancies. They concluded that if the ratio is bigger than 1.4, tissue comprises squamous cell carcinoma or adenocarcinoma (Yano et al., 2000).

FTIR microspectroscopy is also used for analysis of tumor cell invasion. Firstly they made 3D artificial membrane composed of collagen for mimicking the lung basal membrane and then observed the invading cells within this membrane. They clearly stated that the amide A, I and II bands of invading cells were shifted due to the conformational change in the phenotype of cells. This study certified the usability of FTIRM as a fast and reliable method for the screening of tumor cell invasion (Yang et al., 2005).

There are many articles on breast cancer research. Eckel et al. worked on the normal, carcinoma, fibroadenoma and hyperplasia tissues taken from the breast and investigated the spectral patterns of protein originated bands. Some of their results signify that, bands located between 3000-3600 cm^{-1} shift to lower frequencies in carcinoma samples and the absorbance ratio of 3300 cm^{-1} to 3075 cm^{-1} increase in fibroadenoma samples. On the

other hand malignancy decreases the α-helix amide I band frequencies while increasing the β-sheet amide I frequency. Relative collagen content increases due to the malignancy development (Eckel et al. 2001).

Skin cancer is another interesting area for researchers. ATR-FTIR spectroscopy was applied for the determination of hydration in stratum corneum. By measuring the hydration state of the skin, it is possible to infer loss of water in the skin. They applied band fitting over the 4000-650 cm^{-1} spectra and concluded that ATR-FTIR spectra can be used for quantitative measurement of individual band parameters (Lucassen et al., 1998).

Another group applied IR spectroscopy for the exploration of basal cell carcinoma (BCC) characteristics. Spectrum analyses were coupled with the linear discriminant analyses and BCC presented significant differences in terms of nucleic acid and protein content. By LDA analysis three different tissues; BCC, follicle sheath and normal ones could be classified with 98.7% accuracy. On the other hand separation of BCC, squamous cell carcinoma and melanocytic lesions were achieved with 93.5% accuracy via LDA (McIntosh et al. 1999).

A number of groups have been working on gastrointestinal cancers employing spectroscopy. Fujioka et al. could separate normal and malignant gastric tissues with 88.6% accuracy via FTIR (Fujioka et al., 2004).

Another diagnostic research with FTIR was conducted with endoscopic gastric biopsies (Li et al. 2005) and esophagus tissue samples (Maziak et al. 2007) which revealed the potential of technique for the detection of malignancies with high specificity and sensitivity.

Stomach cancer was characterized by ATR-FTIR spectroscopy with the absence of CH and C=O bands, shifting of amide I band to lower wave numbers and the presence of weak amide II band at 1545 cm^{-1}. Also the band intensities and band positions of amide I and II bands show considerable differences between normal and malignant differentiations (Xu et al. 2005).

Structural differentiations in DNA of pancreatic cancer tissue were investigated with FTIR spectroscopy. Isolated DNAs showed significant disorders in phosphodiester - deoxyribose spectral region compared to normal tissue DNA (Kondepati et al., 2006).

1.7.1 FTIR Spectroscopy and Cancer Grading

FTIR spectroscopy have been tried to be developed as a tool for cancer grading by several researchers. Freeze dried lymphoid tumors were investigated with FTIR and the absorbance ratio of the spectral bands on 1121 cm^{-1} and 1020 cm^{-1} was showed increasing

pattern due to the increasing pathological grade of malignant transformation. After this study, the ratio of 1121/1020 cm^{-1} was assigned as an index of cellular RNA/DNA. Also they suggested this ratio as a global cancer grading parameter (Andrus and Strickland, 1998).

Mordechai et al. reported the usage of FTIRM for the follow up childhood leukemia patients. Isolated lymphocytes from the children before and after the chemotherapy were characterized with FTIRM. Significant changes were indicated in the region of 800-1800 cm^{-1}, chemotherapy caused the decrease in nucleic acid, cholesterol and total carbohydrate levels in B and T type acute lymphoblastic leukemia patients (Mordechai, et al., 2001).

Spectra from various grades of non-Hodgkin's lymphoma were analyzed by Andrus and the increase in CH_3/CH_2 ratio along with decrease in sym. CH_2/asym. CH_2 ratio was indicated with increasing malignancy grade. In addition, lymphoma grade correlates with the rising ratio of 996/966 cm^{-1}, which assigned to RNA/DNA ratio, and the increase in the intensity of band 1121 cm^{-1}, that is an index of ribose content (Andrus, 2006). Raman and FTIR spectroscopy in combination with multivariate statistics were applied to esophageal lymph nodes for observing the macromolecular changes during carcinogenesis and metastasis development. These studies revealed that both of spectroscopic techniques are able to correctly separate benign and cancerous tissues from each other with the percentage of 94 via PCA and LDA. It was also indicated that cancer formation yields higher nucleic acid but lower lipid and carbohydrate content, which can be regarded as the signs of loss of differentiation and increased proliferation in cells (Isabella et al., 2008).

1.8 Part II: Botanical Origin Determination of Turkey Honeys

1.8.1 Honey Types

Sensory properties and chemical composition exhibit considerable varieties between different honey types due to the harvesting time, nectar proportions, vegetation type or the species of bee, sucking the plant. In addition, even unifloral honeys can vary depending on the regional differences. There are no established criteria for controlling the botanical designations of honey types. National laboratories of each country try to establish their own analytical standards. This results in complications especially in trading, in terms of the wrong declarations of unifloral honeys (single flower honey). To clarify this situation, for the 15 most important unifloral honeys in Europe, a kind of monograph including the physicochemical, pollen and sensory properties, has been published (Persano Oddo and Piro, 2004).

1.8.2 Universal Theoretical Criteria for the Determination of Botanical Origin

It is not possible to get pure unifloral honey, even if a single plant species are dominated in a particular area. Definition of limits between unifloral and polyfloral honeys is so difficult. After the development of analytical methods, there had been some attempts to procure pure unifloral honeys as a reference. However the relation of these reference samples to the real ones may be problematic. So the new approach which makes possible to differentiate honey groups due to their similar characteristics, will be more promising. Yet, there have been no single method which is able to determine the ratio of different nectars in particular honey sample. With the help of several analytical techniques, only the most dominant nectar source could be estimated.

1.8.3 Conventional Methods for Botanical Origin Determination

1.8.3.1 Pollen Analysis

Pollen constitution projects the vegetation type of honey. Thus, information about the geographical and botanical origin can be inferred. Microscopic evaluation of the pollen reflects the honey extraction method, adulteration (Kerkvliet et al., 1995; Kerkvliet and Meijer, 2000), fermentation (Russmann, 1998) and some beekeeping practices of beekeepers (Louveaux et al., 1978). Pollen grains are examined under light microscope after the sediment preparation by centrifugation. Up to now 500 to 1000 pollen forms have been identified qualitatively. Studies showed that, for frequent pollen types, standard deviation was founded as 3% while it rises up to 45% for rare pollen forms (Von der Ohe et al., 2004). Factors that influence the pollen specialties can be assigned as; the morphology and the physiology of plant, contamination with the pollen of other plants in the hive during pollen processing and contamination during mechanical honey extraction by beekeepers (Ruoff, 2006).

1.8.3.2 Sensory Analysis

Sensory analysis is generally carried out for the identification of impurities, fermentation and the minor amount of off-flavors. Also as a result of sensory analysis conducted by experts, some characteristics that provide the precise determination of botanical origin, was evaluated. Descriptive sensory analytical techniques have been improved and reviewed (Piana et al., 2004). But still most of the experimental methods and statistical analyses have been carried out without any de facto procedure. Sensory analysis might be evaluated as complementary method with pollen analysis. The consideration of similar characteristics which are discerned by the consumer can be advantageous over other methods.

1.8.3.3 Physical and Chemical Techniques

Mostly physicochemical parameters are used for quality detection and honey adulteration. However the sugar composition and electrical conductivity parameters can be used for botanical origin interpretations.

1.8.3.3.1 Electrical Conductivity

Mineral content directly affects the electrical conductivity of honey (Accorti and Piazza, 1987). Experimentally it can be measured with the help of conductometer and regarded as important variable for the categorization of unifloral honey types (Mateo and Bosch, 1998). But, electrical conductivity could not be used as a single parameter for botanical origin determination as it exhibits significant fluctuations within limit values especially for some honey types like, lime, strawberry, chestnut and eucalyptus tree honeys (Krauze and Zalewski, 1991; Piro et al., 2002; Devillers and Morlot, 2004).

1.8.3.3.2 Carbohydrate Content

Approximately 95% of honey is composed of sugars. For the classification of unifloral honey, fructose and glucose level meanwhile the fructose/glucose ratio are important parameters (Persano and Bogdanov, 2004). It was reported that the amount of di and trisaccharide is higher in honeydew honeys. Only glucose, sucrose and fructose are derived from the phloem sap and nectar, the remaining di and trisaccharides are produced by aphids as a result of microbial activity and enzyme catalyzed reactions during honey generation (Bacon and Dickinson, 1957). By the evaluation of minor sugars, only the honeydew and blossom honeys can be differentiated (Sabatini et al., 1990; Mateo and Bosch, 1997; Radovic etal., 2001). But the determination of sugar composition provides higher diagnostic value for botanical origin differentiation for varying kinds of honeydew honeys.

1.8.3.3.3 Water Content

The amount of water is accepted as the most important factor for the determination of honey quality as it is directly associated with the spoilage risk. However it has fairly less importance for the botanical origin characterization. According to the reports, blossom honeys have higher water content than honeydew honeys (Persano and Bogdanov, 2004; Manikis and Thrasyvoulou, 2001). As the water content can be changed during honey processing artificially, this measurand can not be a reliable specifier for botanical origin.

1.8.3.3.4 Color

Lovibond instrument or much simpler Pfund color grader are used for color grading of honey which depends on the basic optical comparison (Fell, 1978). Pfund grader provides continuous amber-colored glass scale which lies from light to the dark. Color intensities are expressed as numbered values and marketed usually according to Pfund color grader scale. For fresh unifloral honey classification, color stated as a useful parameter but the darkening of honey color during storage must be taken into account (Gonzales et al., 1999).

1.8.3.3.5 Optical Activity

Each different sugar molecule in honey represents different optical rotation in response to polarized light. As example glucose exhibits positive rotation while fructose show negative one. Concentration of Dominant sugar type determines the overall rotation of particular honey type (Persano and Bogdanov, 2004; Piazza et al., 1991).

1.8.3.3.6 pH Value

The pH of honey falls within 3.5 and 5.5. Organic acid composition directly determines the pH value in addition to their contribution to the honey stability opposing microbial activity and flavor. Free or total acidity and pH value can be regarded as classification measurands for unifloral honeys (Mato et al., 1997).

1.8.4 Different Alternative Techniques for Botanical Origin Determination

Up to now different methods have been suggested, but none of them has been gained satisfactory acceptance as a single botanical origin identification technique. Some of them are discussed below.

1.8.4.1 Chemometric Approach

Usage of chemometrics for the classification of different honeys has been proposed in previous researches. In 1960 discriminant functions of monosaccharide and ash content in addition to pH values were used for classification (Kirkwood et al., 1960). Later, as a characteristics of flower honey, high concentration values for glucose and fructose and low free acidity, polyphenol content, lactone quantity and electrical conductivity were assigned while the reverse of that measurands were described as characteristic for honeydew honeys (Sanz et al., 2005).

Linear discriminant analysis was employed to select most useful measurands by evaluating the different sugars, water, pH value, color, diastase enzyme activity, conductivity and hyroxymethylfurfural content. And finally, by using pH value, free acidity, electrical conductivity, fructose, glucose and raffinose contents, botanical origin of honeys could be estimated perfectly (Devillers et al., 2004).

1.8.4.2 Volatiles

Volatiles originates from the corresponding plant that the pollen is collected and responsible for the honey type specific flavor (Rowland et al., 1995; Alissandrakis et al., 2003).
For the study of volatile composition, various techniques have been proposed like, steam distillation (Bicchi et al., 1983), solvent extraction (D'Arcy et al., 1997), gas sensor (Ampuero et al., 2004), dynamic headspace extraction (Bouseta et al., 1992). Some volatiles had been recommended as markers for the classification of unifloral honey types. As an example, 2-aminoacetophenone is suggested for chestnut honey marker while methyl anthranilate for orange honeys (Guyot et al., 1998). Instead of single component, the combination of more than one volatile component, give more efficient and promising results (Perez et al., 2002; Soria et al., 2004). However, in the cases where the chromatic separation is used the techniques get long times and the outputs are not reproducible enough. Only the usage of gas sensors, seem to be most convenient and promising approach.

1.8.4.3 Amino acids / Proteins

Proline, the most dominant amino acid in honey is important marker for the determination of honey adulteration and ripening. Also the profiles of free amino acids were suggested as geographical origin determinants (Davies and Harris, 1982; Gilbert et al., 1981). Moreover, previously the concentration difference in tryptophan and glutamic acid were used for the differentiation of blossom from honeydew honeys (Iglesias et al., 2004). For the evaluation of honey proteins alternative techniques like polymerase chain reaction based methods and some immunoblotting assays were developed more recently (Siede et al., 2004; Baroni et al., 2002). Although the sensitivity of these techniques is really high, they suffer from the similar limits as seen in pollen analysis.

1.8.4.4 Spectroscopic Techniques in Botanical Origin Determination

For food industry, Near-Infrared Spectroscopy (NIR) has been accepted as rapid and reproducible technique (Bertrand and Dufour, 2006). In honey analysis both the reflectance and transmission modes have been utilized in the last decade. For a sample group composed of honeys taken from 13 different botanical origins, the discrimination

potential of NIR was evaluated with the help of chemometric analysis. As a result 67% of the samples were correctly grouped in terms of botanical origin while none of them could be assigned to correct class due to their geographical origin (Davies et al., 2002). In another study conducted with limited number of samples composed of only eucalyptus and polyfloral honeys, 75% of the polyflorals and the 85% of the eucalyptus were correctly classified (Corbella and Cozzolino, 2005).

Mid-infrared spectroscopy (MIR) accepted as a more informative technique allowing the collection of more distinct and specific absorption bands, than NIR. But the application of MIR to the honey samples is far less. For the quantification of some measurands collected with MIR, including glucose, fructose, sucrose and maltose content, electrical conductivity and pH value, partial least square (PLS) model were developed. A disadvantage of this method is the usage of semi-automatic instrument. MIR spectroscopies are basically designed for the analysis of liquids so honey samples must be liquefied with water, contained a specific liquid called "Zero Liquid (FOSS, Hillerod, Denmark)", which causes significant noise due to water absorption (Lichtenberg-Kraag et al., 2002). To overcome this, usage of ATR accessory come into prominence. In previous study, glucose, sucrose, fructose and maltose were analyzed with ATR-FTIR in 60 honey samples in addition to pure sugar solutions. Calibration model was developed as a result of PLS analysis for the evaluation of sugar concentration. As a reference method, HPLC was used for the calculation of correlation coefficients and according to information gathered, ATR-FTIR allows accurate and rapid quantitative analysis for honey (Tewari and Irudayaraj, 2004). Recently ATR-MIR was proposed as a promising tool for botanical origin determination. When the display of spectra was observed, it was seen that the difference was observable in absorption level rather than shape. However by using linear discriminant scores, the success of grouping of samples was not satisfactory (Tewari and Irudayaraj, 2005).

1.8.4.4.1 Raman spectroscopy

In Raman spectroscopic approach, laser light in the NIR region, is utilized for the determination of honey adulteration (Paradkar and Irudayaraj, 2002). When the Raman spectroscopy was coupled with neural network analysis, 13 out of 14 honey samples could be placed in correct classes (Goodacre et al., 2002). Nevertheless, theoretically it can be said that, Raman and near infrared spectroscopies have the same potential for botanical origin determination tasks.

1.8.4.4.2 Fluorescence spectroscopy

Fluorescence spectroscopy provides 100 to the 1000 fold higher sensitivity by using the fluorescence emission than the other absorption based spectroscopic methods. It gives a way to the collect information related with the fluorescent molecules and their

microenvironments. Food samples contain number of fluorophore molecules which causes overlapping signals during measurement. Nevertheless, the overall spectra can be used for identification of foods when coupled with multivariate statistical analysis. Polyphenols (Ferreres et al., 1993) and some aromatic amino acids (Bogdanov and Martin, 2002) in honey show strong fluorophore speciality and proposed as classification markers.

1.9 Basis of Infrared Spectroscopy

1.9.1 Electromagnetic Radiation

There is always an electrical field around the static electrical charge. This field applies the pushing and pulling forces to the electrical charge rather than the in prospected electrical charge. If the static electrical charges move, it forms a magnetic field around itself. The resultant force of these electrical and magnetic fields assigned as the electromagnetic field. When the electrical charge move with acceleration, the electromagnetic field of the electrical charge forms the electromagnetic wave and conducts energy called as electromagnetic radiation. If the charges oscillating periodically, the electrical and magnetic components of the electromagnetic field, vibrate perpendicular to the each other and also the direction of propagation of the wave (Nasuhoglu & Tokmacioglu, 1969). Electromagnetic radiation has particle, wave duality. Specialities of electromagnetic radiation like; frequency (v), wave number (λ), period (T) and the amplitude can be examined with classical sinusoidal wave model (Figure 1-2) (Skoog et al, 1998).

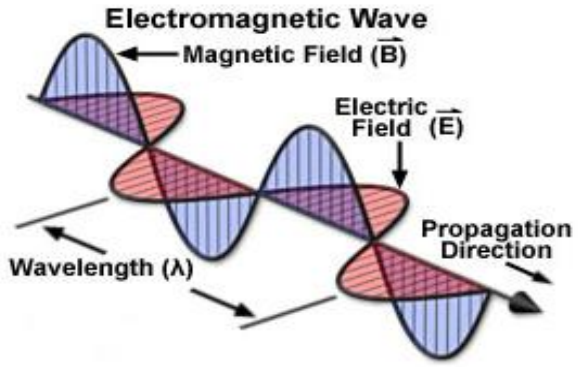

Figure 1-2 Representation of electromagnetic wave (Retrieved from http://micro.magnet.fsu.edu/primer/java/electromagnetic/ , on 5 June 2013)

1.9.1.1 Regions of Electromagnetic Spectrum

Maxwell equation says that, energy is conducted as electric and magnetic waves in the vacuum. As the electromagnetic waves are propagated with the velocity of light c (=$3x10^8$ m/s), the relationship with the v and λ can be represented with the formula (1);

$$\lambda = c/v \quad (1)$$

(Hollas, 2002)

"Electromagnetic radiation is composed of the radio wave, microwave, infrared, visible part, ultraviolet, x-ray and gamma-ray" as represented in Figure 1-3.

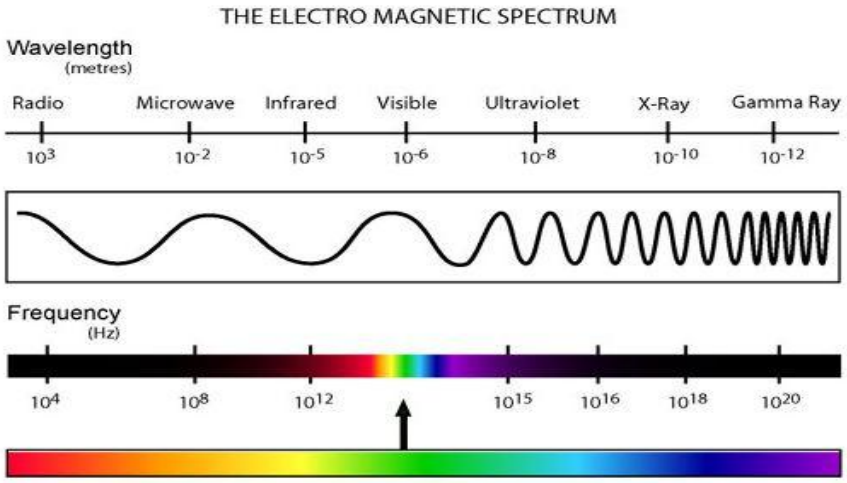

Figure 1-3 The electromagnetic spectrum (Retrieved from http://zebu.uoregon.edu**,** on 5 June 2013)

1.9.2 Molecular Spectroscopy

Molecular spectroscopy investigates the interaction of electromagnetic radiation with the molecule. When the molecules interact with photons, they turn into excited phase by absorbing the energy of photons but then they try to recover this unstable state by distributing excess energy. As a result of this, it can be possible to gather physical and chemical information related with the, molecular symmetry, bond length, bond angles, bond strength, inter and intra molecular forces (Skoog et al, 1998).

According to the Born-Oppenheimer approach, total energy of a free molecule defined as;

$$E_{total} = E_{rotation} + E_{vibration} + E_{electronic} + E_{translation} + E_{electron\ spin\ orientation} + E_{nuclear\ spin\ orientation.} \quad (2)$$

Electromagnetic spectrum is divided into regions depending on the wavelength and frequency properties of the electromagnetic radiation. The electromagnetic spectrum regions and the spectroscopic techniques related to each region are given with the wavelength range values in Table 1-4 (Chang, 1971).

Table 1-4 Electromagnetic regions and attributed spectroscopic techniques.

Region	**Wavelength**	**Spectroscopic technique**
Radio-wave region	10m – 1m	NMR & ESR spectroscopy
Microwave region	1cm - 100μm	ESR spectroscopy
Infrared region	100μm - 1μm	Vibrational spectroscopy
UV-visible region	1μm – 10nm	UV-VIS spectroscopy
X-ray region	10nm – 100pm	Electronic transitions in inner shells
γ- ray region	100pm – 1pm	Nuclear transitions

Vibrations and the transitions between rotational energy levels are examined in the infrared region.

1.9.2.1 Vibrational Spectroscopy

Vibrational spectroscopy techniques principally depend on the light scattering/absorption phenomena, used for the investigations of internal structure of molecules. At the beginning, techniques have been commonly used in chemistry however it has been chosen as a powerful tool for biological studies as the detailed information of spectra gathered from biomolecules allows the determination of subtle changes. In theory, any pathological, physical or physiological changes in the molecule ended up in changes of native biochemistry of molecule so these changes can be detected in Fourier transform

infrared (FTIR) and Raman spectra. These techniques allow the identification of chemical bonds and functional groups of cells or tissues which eventually leads to the monitoring of macromolecular changes including proteins, carbohydrates, lipids and nucleic acids (Diem et al., 2008)

1.9.2.1.1 Molecular vibrations

Atoms in any molecule are always in motion relative to one another, thus bond lengths and planar locations of atoms can be changed. The collection of these kinds of kinetic variations, are called as molecular vibrations (Stuart, 2004). Main types of molecular vibrations are summarized as in the Figure 1-4 below:

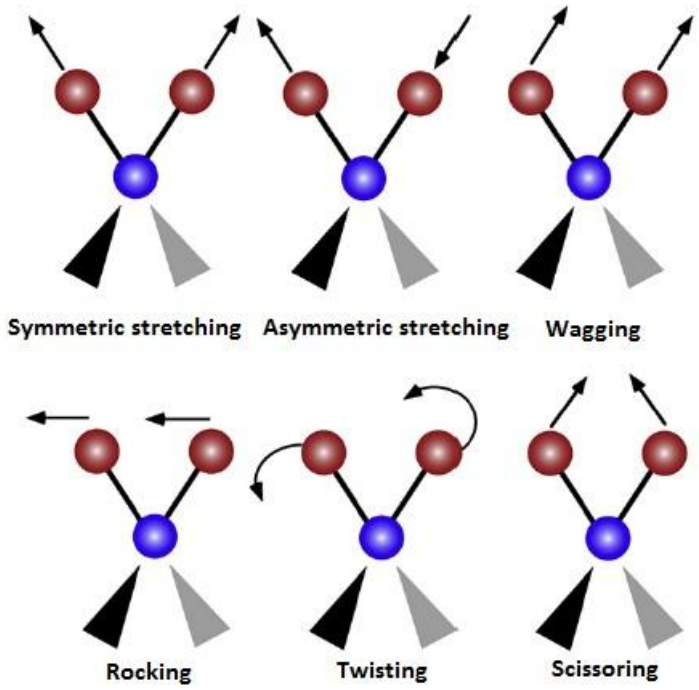

Figure 1-4 The vibrational modes associated to a molecular dipole moment change detectable in an IR absorption spectrum (Adapted from Marcelli et al., 2012).

1.9.2.2 Principals of FTIR Spectroscopy

When infrared radiation interacts with matter, radiation is absorbed and leads to the excitation of molecules into the higher vibrational levels. Chemical bonds vibrate at

characteristic frequencies. Each sample can absorb specific characteristic infrared wavelength due to its molecular structure. A molecule or a bond must have a dipole moment in order to be IR active. So it can be said that IR spectroscopy is used for the detection of changes in dipole moment.

Electromagnetic radiation can behave as a wave or particle. Infrared radiation also has an electromagnetic origin. The energy of this radiation can be written as (formula 3);

$$E=hv \quad (3)$$

Where h denotes the Planck's constant and v refers the frequency. In a typical infrared spectrum, the absorption of a radiant versus wavenumber (cm^{-1}) is plotted. The location of absorption peaks and the amount of radiation that is absorbed are important parameters for molecular investigations.

A beam of infrared light passes through the sample and eventually the changes at energy levels of photons of sample are recorded as a spectrum. To achieve this monochromatic light which changes in wavelength during time must be used. But by using Fourier transformation instruments, it is possible to record all the wavelengths at once.

FTIR spectrometer is based on the Michelson Interferometer which uses the beam splitter for taking the incoming IR light and dividing it into two optical beams. Then one beam goes to a fixed flat mirror while the other one goes to a moving flat mirror which moves a few millimeters away from the beam splitter. Two beams recombine at the beam splitter after reflection (Figure 1-5). These two beams interfere with each other and the resulting signal is called as interferogram (Gerwert and Kötting, 2010). Every data point in a single interferogram carry the information related with every infrared frequency coming from the source. By measuring the interferogram, all the frequencies are being measured simultaneously this gives the advantage of highly fast measurements. Fourier transformation is a mathematical function, used for the convertion of interferogram into intensity versus frequency spectrum, for the interpretation of signals.

A background spectrum is taken for relative scaling of absorption intensity. Then this background spectrum is compared with the spectrum of the sample of interest to determine the "percent transmittance" and to remove the instrumental characteristics and finally to get pure spectrum where all the signals are due to the sample.

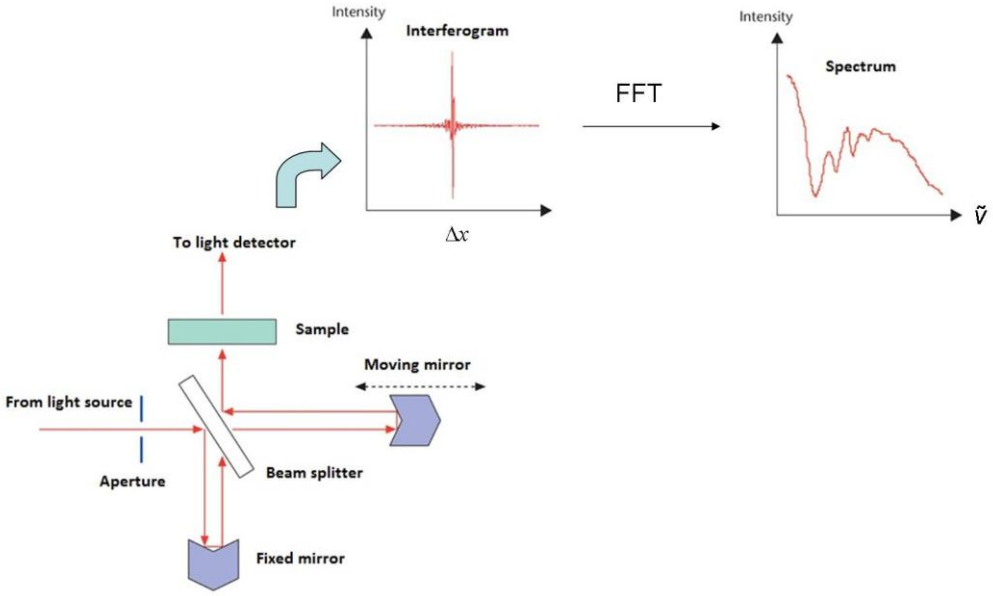

Figure 1-5 Typical setup of a Fourier transform infrared (FTIR) spectrometer (Retrieved from Gerwert and Kötting, 2010).

FTIR spectroscopy is a potential tool for non-invasive, practical optical diagnosis. Currently it has become important reliable analytical methods for biomedical investigations. Measurements with FTIR can be conducted with non-destructive approach and samples with quite small quantities can be enough for analysis. The basic specialities of FTIR can be summarized like in the Table 1-5 below:

Table 1-5 FTIR basics

Sample properties	Non- aqueous samples
Sample preparations	Little or no sample preparation in photo acoustic sampling techniques
Materials can be analyzed	Certain inorganic molecules, mostly organic molecules can be analyzed. In addition, synthetic and natural compounds can also be analyzed.
Physical effect of technique	Depends on absorption phenomena, analyses the changes in dipole moment of molecules.
Resolution limits	Varies within 1 – 20 μm due to the beam splitters.
Frequency range	4000-200 cm^{-1} for Mid-IR.
Problems of technique	Water absorption has strong signal so creates problems in analysis

1.9.2.2.1 Attenuated Total Reflectance Fourier Transform Infrared (ATR-FTIR) Spectroscopy

In the attenuated total reflection mode, the changes in the totally internally reflected beam is measured when the IR beam contacts with the sample. An optically dense crystal with high refractive index was placed in front of the IR beam with a fixed angle to create internal reflectance. As an ATR crystal, diamond, zinc selenide (ZnSe), germanium and silicon or amorphous material transmitting IR (AMTIR) are preferred due to their high refractive index. Created evanescent wave extends into the sample which is placed onto the crystal up to 0.5μ to 5μ. Evanescent wave is being attenuated when the sample absorbs the related spectral energy. Then attenuated energy is passed back to the IR beam and leaves the crystal from opposite end and finally reaches the detector to generate the infrared spectrum (Figure 1-6).

The operation of technique depends on some basics: sample must be in contact with crystal, refractive index of ATR crystal must be remarkably greater than the index of sample (Perkin Elmer Life Sciences, 2005; Kazarian *et al.*, 2006).

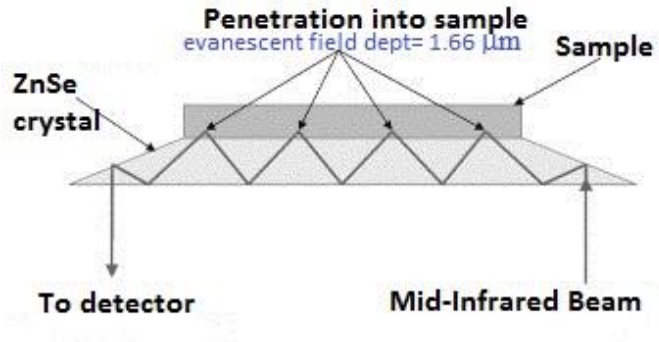

Figure 1-6 Schematic representation of ATR attachment's top plate, (Retrieved from Ellis and Goodacre, 2001).

Advantages of ATR Technique

ATR provides constant path length for every independent sample since a wave can penetrate up to a limited distance beyond the crystal surface (Cocciardi et al., 2005).

Sample preparation step is easier for both liquid and solid materials when compared to transmission mode FTIR.

Conne's Advantage in FTIR Spectroscopy

In FTIR spectroscopy, we cam detect very small changes in frequency shifts or area values sensitively. All FTIR's use analog to digital converters to convert the voltage of detector, into digital signals, to make them interpretable by software of the system. External trigger input of these converters, determines the sending time of digital signs to the computer. He-Ne laser of reference interferogram always generate these external triggers. Principally, this technique provides the acuurate and precise referencing of all the wavelengths of measured IR spectrum to the HeNe laser's wavelengths which are consideranly stable. This advantage of the technique is called as "Conne's advantage". With the help of this advantage, FTIR spectrometers able to provide a wavelength accuracy specification which is better than 0.01 cm^{-1}, although user select 1, 2 or 4 cm^{-1} resolution (Perkins, 1987).

1.10 Chemometrics in Biospectroscopy

Spectra of biological samples contain hundreds of varying absorbance intensities at each specific wavenumber. In an investigated sample group, huge number of spectra is acquired and these data varies not only between classes but also within classes especially in biological systems. At that point, multivariate data analysis come into prominence which

have advantage over univariate analyses techniques, that only allowing the detection of variations between classes. Statistical data analyses have two main aims: making more global exploration over data and classification of samples. Exploratory analysis helps the interpretation of biochemical variations related to classes in whole data while the classification techniques foresee spectroscopy as an applicable screening and diagnosis tool.

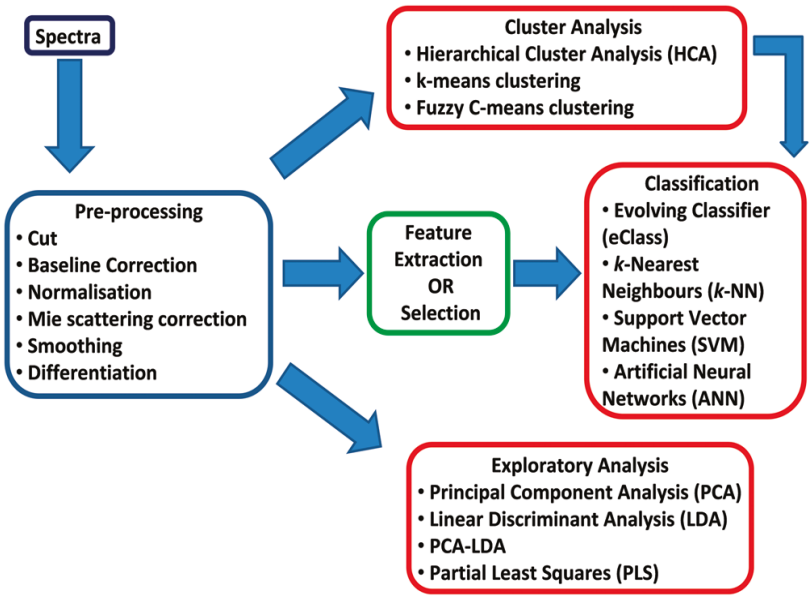

Figure 1-7 Overview of possible ways for computational data analysis after the collection of spectral data pool (Retrieved from Kelly et al. 2011).

1.10.1 Pre-processing

Spectral data are subjected to pre-processing in order to get rid of noise, to correct baseline slope and thickness differences between samples and also for the selection of the region of interest. Preprocessing generally composed of baseline correction, normalization and cutting as indicated in Figure 1-7.

Theoretically wavenumbers which have not been absorbed by the sample of interest should have a zero absorbance. But, in some regions especially in the fingerprint region, infrared spectra raises above the point of zero absorbance due to the Mie scattering, temperature, concentration or instrumental anomalies. Anomalies in baseline can be removed by variety of correction techniques provided by software which stretches the

spectrum down thus minima areas fit a convex line. This polygonal line is then subtracted from the raw spectra. Normalization is generally preferred to show the variations visually. Minimum or maximum normalization can be used when a particular peak is stable among all specimens. In some circumstances, vector normalization may be used by which each spectrum is splitted by its Euclidean model (Kelly et al. 2011).

1.10.2 Principal Component Analysis

Commonly used multivariate analysis methods like Principal Component analysis (PCA) and Partial Least Squares (PLS) are preferred in spectroscopy for decoding the spectra containing overlapping regions (Levin and Bhargava, 2005).
Multivariate techniques able to differentiate the spectra in a properly selected spectral range, using the correlation level between the change, occurring on interested variables and collected data. Thus, all the data on a spectrum reduced to principal components (Martin and Pollock, 2010). PCA applies linear transformation to the wavenumber data via PCA loading matrix. Loading vectors namely principal components in loading matrix are eigenvectors. A variable called "PCA factor" is generated by the linear combination coefficients of each principal component. As the principal components are orthogonal to each other, they are uncorrelated. Eigenvalues of each principal component match with the variance of their related PCA factor. If three principal components are selected and spectra are plotted in PC space, that has been linearly transformed, each spectrum is represented as a single point in three dimensional spaces. Generally first 3 principal components are preferred since they comprise the vast majority of variance thus allowing the optimal representation of data (Korenius et al., 2007).

1.10.3 Hierarchical Cluster Analysis

Cluster analysis is also a kind of un-supervised multivariate analysis technique which principally groups the samples based on their characteristic specificities. Similar samples tend to be classified in a same group in clustering. Dendrograms are used for the visualization of clustering. Differences between the clusters are indicated with heterogeneity values.

In data analysis, primarily usage of techniques like PCA, can be useful for the determination of general relationship web among data. However, cluster analysis must be performed if one wants to show grouping of similar data gathered from different samples. (Kazarian and Chan, 2006).

CHAPTER 2

MATERIALS AND METHODS

2.1 Study I

2.1.1 Patients

A total of 70 individuals who were diagnosed with bladder tumor during clinical screening were recruited to this study, of whom 7 were women (10%) and 63 (90%) were men. Some of the patients come to the clinic with tumor recurrence while in case of some of them, no tumor recurrence has occurred. Criteria, satisfied by patient for recruiting our study, were as follows;

- The histopathologically proved presence of bladder tumor
- No malignancy related with any other urethelial system organs rather than bladder
- Overall evaluation of bladder with cystoscopy
- No intercavitary treatment application to the patient within six months

Patients were divided to four groups as a result of pathological investigation and cystoscopy:

- Control group (n=21) which has normal bladder epithelial tissue;
- Papilloma group (n=2) which has uretelial papilloma;
- PUNLMP group (n=3) which has uretelial neoplasm with lower malignancy potential;
- Carcinoma group (n=44) which has low and high grade papillary uretelial carcinoma.

All procedures used in the experiments were approved by the Ethics Committee of Tepecik Eğitim ve Araştırma Hastanesi, İzmir, Turkey (Ethics Committee meeting in 30.03.2007, and decision no: 8).

2.1.2 Sample Preparation

The following steps were carried out for the detection of bladder tumor via ATR-FTIR spectroscopy;

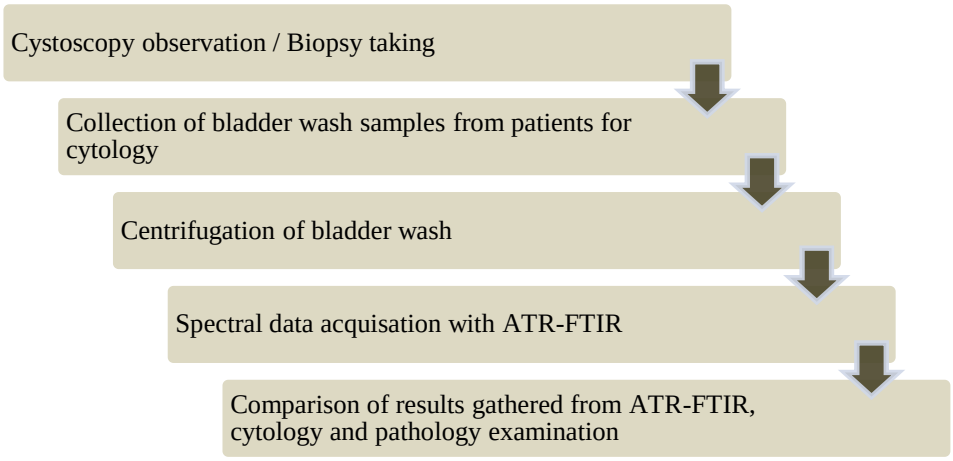

First step was to collect the bladder wash samples from the patients. During cystoscopy, bladder tissue was observed with the camera; tissue biopsy was taken from the suspected area and sent to the pathologist. Also the bladder wash sample of 10 ml was collected for cytology. Then samples were centrifuged for 30 minutes at 10,000 rpm. After the removing of supernatant the remaining pellet was used for urine cytology examination. The pellet left was stored at -80 ^{o}C until ATR-FTIR analysis.

Finally the results coming from biopsy and urine cytology were compared with the results of ATR-FTIR.

2.2 Study II

2.2.1 Honey Samples

A total of 111 honey samples were collected from different geographical regions of Turkey. Samples were purchased commercially either from well-known brands or directly from beekeepers. Flower originated (polyfloral, anzer, organic, mountain flower), tree originated (pine, chestnut, cedar) and rhododendron honey samples and additionally maple syrup, fructose syrup and grape molasses samples were included to the study. The sample size of each group is indicated in Table 2-1:

Table 2-1 Investigated sample groups, number of samples were indicated as 'n'.

<table>
<tr><th>Tree originated</th><th>Flower Originated</th><th>Rhododendron</th><th>Other Samples</th></tr>
<tr><td rowspan="2">Chestnut Honey (n=10)</td><td rowspan="2">Polyfloral Honey (n=30)</td><td rowspan="4">n=30</td><td>Maple syrup (n=3)</td></tr>
<tr><td rowspan="2">Fructose syrup (n=3)</td></tr>
<tr><td rowspan="2">Pine Honey (n=20)</td><td rowspan="2">Anzer Honey (n=3)</td></tr>
<tr><td>Grape Molasses (n=3)</td></tr>
<tr><td rowspan="2">Cedar Honey (n=3)</td><td rowspan="2">Organic flower Honey (n=3)</td><td>Adultered Honey (n=3)</td></tr>
</table>

Honey samples were grouped as tree and flower originated ones basically.

Chestnut honey is produced from both nectar and secretum collection by honey bee.
Pine honey is kind of honeydew honey, produced via using the secretum of insect, living in the trunk of pine tree, by bees. Pine honey is specific endemic product, can be found only in Turkey and Greece.
Cedar honey, used in this study, was collected from the Toros Mountains in the Mediterranean region of Turkey, and mainly originated from Cedar trees.

Flower originated group is composed of polyfloral honeys collected from different regions of Turkey, in addition to Anzer and Organic honeys. Anzer and organic flower honeys are produced specifically in the plateaus of Black Sea region, and rich in nectar and pollens coming from many endemic flower species.

Rhododendron honey, locally called as "mad honey" or "toxic honey", collected from the nectars of rhododendron species. Rhododendrons are mainly growing in the eastern Black Sea Region of Turkey. It is phenolic content and antimicrobial activities are quite different from the other honey species.

Maple syrup produced from the xylem sap of maple tree and contains primarily sucrose and water so it was used as a glucose control in this study. Also we have used a fructose control which was purchased from the market as fructose syrup, composed of mainly fructose and water in addition to minute amounts of other carbohydrates. Grape molasses is a traditional sweaty, produced by boiling of the pressed grape juice and special grape soil mixture. It is rich in both carbohydrates and minerals like calcium, potassium, magnesium, chrome and iron.

2.3 Methods

2.3.1 Data Collection with ATR-FTIR

Spectra from all samples were collected in the one-bounce ATR mode in a Spectrum 100 FTIR spectrometer (Perkin- Elmer Inc., Norwalk, CT, USA) equipped with a Universal ATR accessory. Samples were placed on Diamond/ZnSe crystal plate (Perkin-Elmer) directly and scanned from 4000 to 650 cm^{-1} for 100 scans for each interferogram with the resolution of 4 cm^{-1} at room temperature. Spectrum of atmospheric vapor was taken as a background spectrum and subtracted from the all spectra automatically. Data manipulations and calculations were carried out via Spectrum 100 software (Perkin-Elmer). Band frequencies were determined from the raw data frequencies, corresponding to the center of weight. Then band areas were calculated from the baseline corrected spectra.

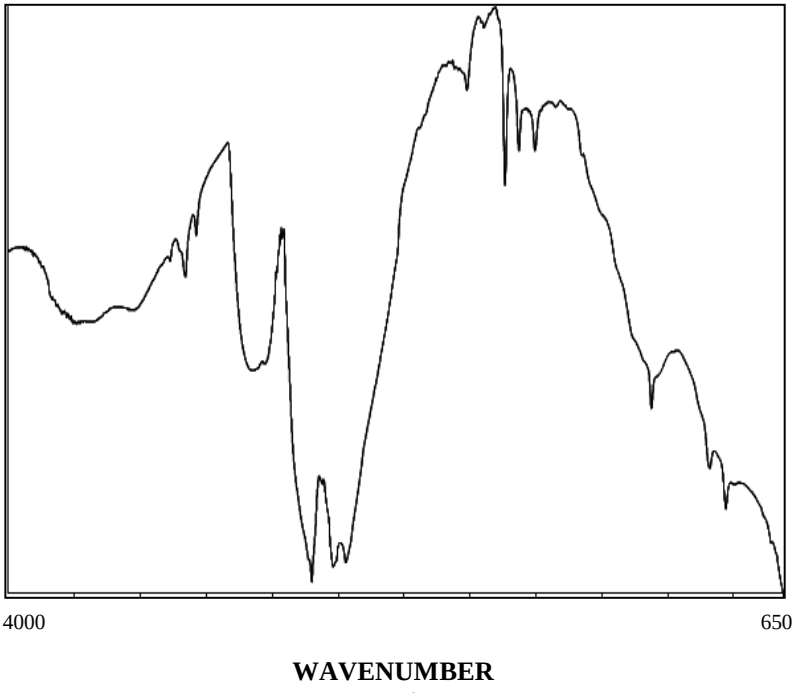

Figure 2-1: ATR-FTIR spectrum of air.

2.3.2 Spectral Data Analysis

Spectral pre-processing was applied to all spectra to make the data set comparable with each other, before starting up of the spectral data analysis. Baseline correction was

performed to correct sloping baseline. In the calculation of band area values, baseline corrected spectra were taken into account. However for the measurement of band frequency values, raw spectra were considered. Center of the weight of interested peaks were determined as the corresponding frequency values of the peaks. Non-normalized and pre-processed average spectra were used for all the quantitative analysis. But only for visual representation, average spectra of each group were normalized to show differences among specific bands.

2.4 Chemometrics

Hierarchical Clustering and Principal Component Analysis were applied to classify the samples based on spectral differences. For the determination of spectral differentiation among studied groups, cluster analysis was performed via nine smoothing point Savitzky-Golay algorithm provided by OPUS 5.5 software (Bruker Optics, GmbH).
To evaluate the success of discrimination, the sensitivity and specificity of the technique were calculate for each examined region. Sensitivity and specificity are commonly used parameters for the performance evaluation of the method.By means of sensitivity, calculation shows the actual positives while specificity indicates the proportion of actual negatives. Optimal prediction is achieved with 100% sensitivity (by not predicting anybody from the healthy control group, as a diseased person) and 100% specificity (by predicting every single individual from the carcinoma group as a cancer) in theory.

For honey data, vector normalized, first derivative of each spectrum in the range of 1800 to 750 cm^{-1} was used as an input. Spectral distances were calculated between pairs of spectra. Pearson's correlation coefficients and Euclidean distance was used to calculate the sample similarities. To indicate the complete linkage clustering Ward's algorithm was used.

Mean-centered Principal Component Analysis was conducted on the ATR spectra of honey groups over the range of 4000-650 cm^{-1} and 1700-1600 cm^{-1} by MATLAB software.

2.5 Statistics

Statistical data analysis and graphing were performed using the GraphPad Prism 5 software package (La Jolla, CA, USA). All samples firstly subjected to Kolmogorov-Simirnov normality test. None of the sample group is normally distributed. Therefore non-parametric tests were preferred for significancy analysis.

In bladder cancer detection study, to compare carcinoma and control samples, non-parametric Mann-Whitney U test was used for the calculation of significancy level.

For making the comparison between groups in the honey classification study, as the

number of groups was more than two, One-way Anova was used. As a post – hoc test to see binary comparisons, Tukey test was preferred. A p-value of less than 0.05 was indicated as significant ($p<0.05$*, $p<0.01$**, and $p<0.001$***).

CHAPTER 3

RESULTS AND DISCUSSION

3.1 Study I: Bladder Cancer Diagnosis from Bladder Wash Sample

This study was conducted for investigating the molecular differentiations during bladder carcinogenesis and also for the development of a new method for bladder cancer diagnosis using ATR-FTIR spectroscopy.

Bladder wash samples were taken from the patients during cystoscopy. Bladder wash liquid is composed of mainly urea, uric acid, creatinine, several different types of cells, some crystal and resectisol (isotonic serum solution used for washing of bladder). As the number of patients in PUNLMP and Papilloma groups was small for statistics, they were not taken into consideration throughout the analysis.

3.1.1 Molecular Investigation

3.1.1.1 Spectral Comparisons of Control and Carcinoma Patients

Infrared absorption bands correspond to the presence of particular groups of atoms in the sample of interest. In Figure 3-1, representational infrared spectra snapshot of bladder wash belonging to healthy patient, is shown.

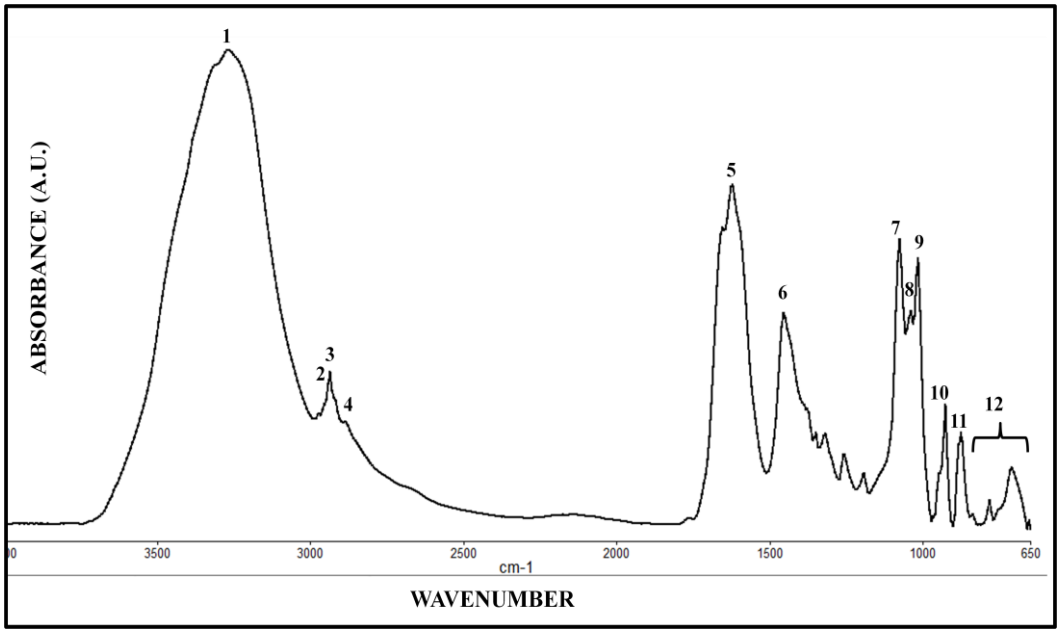

Figure 3-1 Representational ATR-FTIR spectrum of bladder wash in 4000-650 cm^{-1} spectral region

ATR-FTIR spectra of bladder wash samples imply the presence of so many different functional groups of not only organic but the inorganic compounds as well. The frequency positions and the related assignments of some important bands are given in Table 3-1. Band assignments were adapted from previous studies (Rigas *et al.*, 1990; Wong *et al.*, 1991; Wong *et al.*, 1993; Takahashi *et al.*, 1991; Naumann *et al*., 1991; Wang *et al.*, 1997; Jamin *et al.*, 1998; Melin *et al.*, 2000; Jackson *et al.*, 1998; Chiriboga *et al.*, 2000; Cakmak *et al.*, 2003, Cakmak *et al.*, 2006; Toyran *et al.*, 2006; Raunier et al, 2003; Aydin O. Z., 2009).

Mansfield *et al.* (2005) reported that urea shows dominant absorption bands in urine. However the bladder wash sample was subjected to 30 minutes centrifugation, so the sample used was poor in urea, uric acid and creatinine than native samples.

Table 3-1 Assignments of important bands of bladder wash sample.

Band Number	Frequency (cm^{-1})	Assignments
1	**3270**	**N-H and O-H symmetric stretching (Amide A band)**
2	**2955**	**CH_3 asymmetric stretching (from lipid acyl chains)**
3	**2934**	**CH_2 asymmetric stretching (from lipids)**
4	**2886**	**C-H stretching (from lipid acyl chains)**
5	**1628**	**C=O stretching (lipids), Amide I region (proteins)**
6	**1452**	**CH_3 bending (from methyl groups of proteins)**
7	**1076**	**PO_2^- symmetric stretching (from phosphodiester bonds)**
8	**1047**	**C-O stretching (mainly from carbohydrates)**
9	**1020**	**C-O bending (Carbohydrates and DNA)**
10	**927**	**Left handed DNA helix**
11	**872**	**DNA (Z form)**
12	**800-650**	**Fingerprint Region (out of plane bending vibrations)**

With the help of frequency readings it is possible to gather information about the conformation of molecules as well as the intermolecular interactions. On the other hand, band area readings shed light on the concentration level of the molecule of interest. Particularly, in this study for the investigation of bladder cancer induced compositional and conformational changes in molecular level; infrared spectra of bladder wash samples were subjected to detailed spectral analysis in the regions of 3800-3000 cm^{-1}, 2995-2800 cm^{-1} and 1800-650 cm^{-1} as given in Figure 3-2, Figure 3-3, and Figure 3-4 respectively.

Table 3-2 Summary for band frequency analysis of control and carcinoma groups. The values are denoted as Mean ± Standard deviation. Significance degree is shown as * for p <0.05.

Frequency (cm^{-1})			
Band	**Control (n=21)**	**Carcinoma (n=44)**	**Degree of significance**
1	3275.09±4.72	3273.67±5.46	ns
2	2954.53±3.16	2956,79±3.53	p<0.05*
3	2935.84±1.97	2933.62±3.7	p<0.05*
4	2886.11±1.68	2883.75±4.86	p<0.05*
5	1624.61±2.95	1627.95±5.78	ns
6	1453.09±3.44	1452.15±2.53	p<0.05*
7	1076.38±4.33	1078.06±3.34	p<0.05*
8	1046.91±3.94	1047.84±3.6	ns
9	1019.67±3.52	1022.14±4.11	p<0.05*
10	927.80±2.15	927.02±2.41	ns
11	873.31±3.51	871.90±3.96	ns
12	781.07±1.79	781.22±1.88	p<0.05*

Table 3-3 Summary for band area analysis of control and carcinoma groups. The values are denoted as Mean ± Standard deviation. Significance degree is shown as * for $p < 0.05$, ** for $p<0.01$ and *** for $p<0.001$.

Area			
Band	**Control (n=21)**	**Carcinoma (n=44)**	**p values**
1	92.09±28.09	80.9±23.49	p<0.05*
2	1.76±0.78	1.39±0.45	p<0.05*
3	1.78±0.86	2.4±0.9	p<0.01**
4	2.6±1.38	1.9±0.74	p<0.05*
5	18.48±7.8	27.46±16.85	p<0.05*
6	7.36±2.9	9.63±4.1	p<0.05*
7	4.24±1.9	5.49±2.38	p<0.05*
8	2.21±0.7	1.83±0.75	p<0.05*
9	3.73±2.09	4.46±1.63	p<0.05*
10	2.00±1.18	2.90±1.53	p<0.05*
11	2.01±1.32	1.28±1.02	p<0.05*
12	0.42±0.23	2.70±2.9	p<0.001***

3.1.1.1.1 Spectral analysis of 3800-3000 cm^{-1} "Amide A" region

In Figure 3-2, spectra belonging to control and carcinoma groups were normalized with respect to amide A band and shown in the region of 3800-3000 cm^{-1}.

Amide A indicates the N-H and intermolecular O-H stretching absorptions (Cakmak *et al.*, 2006; Melin *et al.*, 2000). As the Figure 3-2 and detailed frequency analysis show, changes were not significant between control and carcinoma groups.

In this study, bulk water was eliminated totally with nitrogen gas drying. So vibrations coming from bulk water to amide A band could be neglected. In this band only intra water band appears as a shoulder around 3500 cm^{-1}. However so many compounds also contribute the absorption of this band like urea, creatinine and some polysaccharides that are specific for our case. Especially urea concentration is easily affected by the diet of patient or the performance of kidneys. So this band does not reflect valuable information about carcinogenesis and therefore was not taken into consideration.

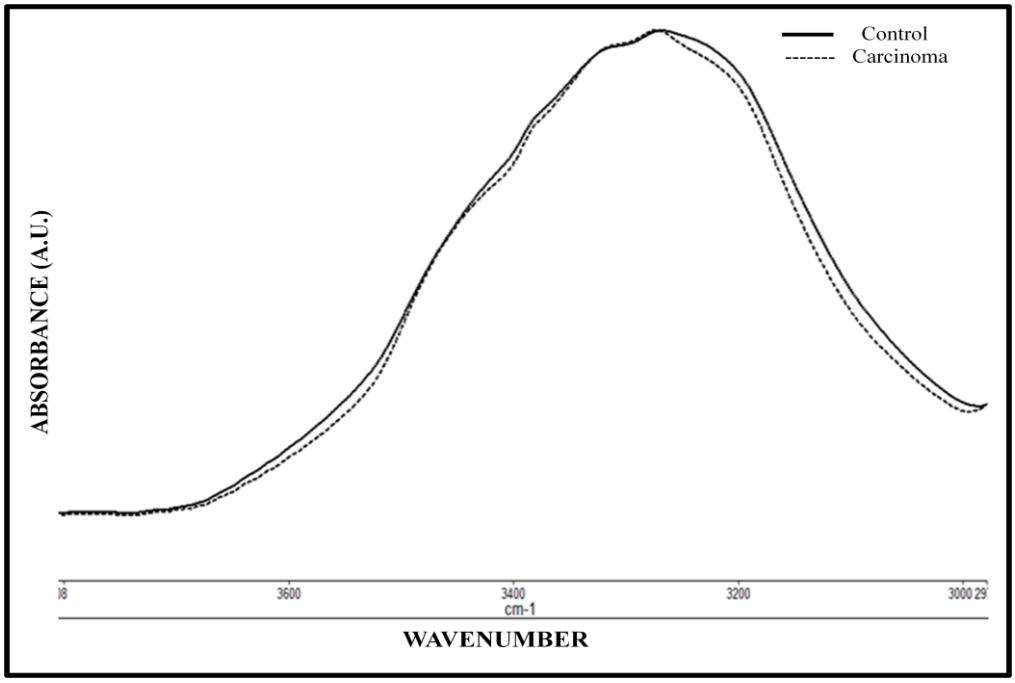

Figure 3-2 Average normalized spectra of control and carcinoma groups in the 3800-3000 cm^{-1} spectral region

3.1.1.1.2 Spectral analysis of 3000-2800 cm^{-1}, "C-H" region

Infrared spectra of control and carcinoma groups in the 3000-2800 cm^{-1} region are presented in Figure 3-3. The spectra were normalized according to the CH_2 asymmetric band which is located approximately at 2936 cm^{-1}. This region specifically called as CH region containing the CH_3 symmetric and asymmetric in addition to CH_2 asymmetric stretching absorptions.

The area of CH_2 asymmetric stretching band shows significant $p<0.01$** increase in carcinoma group compared to control. Vibrations in this band predominantly monitor the overall average trans/gauche isomerization (Mantsch *et al.*, 1984; Severcan, 1997).

The band located at around 2955 cm^{-1} and assigned as CH_3 asymmetric stretching showed cancer induced significant frequency shift to the higher values with $p<0.05$* (Table 3-2). This might imply the increase in the acyl chain freedom in the centre of lipid bilayer membrane in malignant samples. It was known that cancer development influence membrane structure and function. Changes could be held on different lipid rafts in different levels. Changes in the CH_3 asymmetric stretching vibrations evaluated for the monitoring of changes in the deep interior part of phospholipid bilayer (Umemura *et al.*, 1980).

The band located around 2886 cm^{-1} corresponds to the CH_3 symmetric stretching mode sourced mainly from proteins (Melin *et al.*, 2000; Cakmak *et al.*, 2003). There is a significant observable shift in frequency of this peak to the lower values in carcinoma group indicating conformational changes in protein structure.

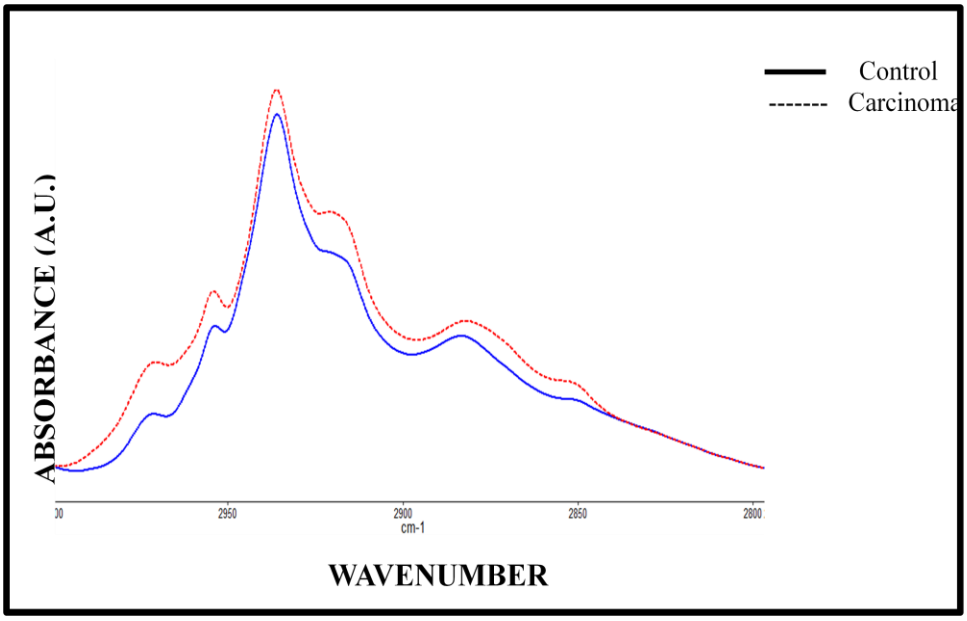

Figure 3-8 Average normalized spectra of control and carcinoma groups in 3000-2800 cm^{-1} spectral region

Bandwidth calculations of CH_2 asymmetric band located at around 2936 cm^{-1}, is used as a metric for membrane dynamics. Differences in bandwidths between same amounts of samples show the changes in membrane fluidity of these compared systems (Mantsch *et al.*, 1984). According to results shown in Table 3-4, there was a considerable tumoriogenesis induced change in the membrane dynamics of carcinoma group (Figure 3-4). Carcinoma group's bandwidth value is significantly higher indicating more fluid membrane structure than the control samples.

Table 3-4 Summary for bandwidth analysis of control and carcinoma groups. The values are denoted as Mean ± Standard deviation. Significance degree was shown as ** for $p < 0.01$

Bandwidth			
	Control	Carcinoma	p-value
CH_2 asymmetric stretching	13.87 ± 5.54	19.09 ± 5.94	p< 0.01**

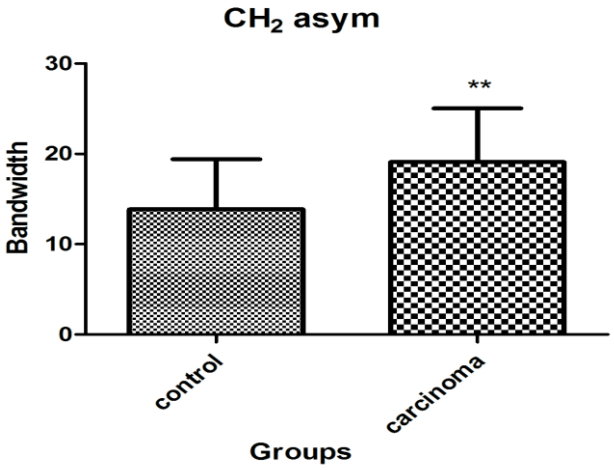

Figure 3-4: Comparison of bandwidth values of CH_2 asymmetric band between control and carcinoma groups. (*) denotes the significancy compared to control samples. The *p* values less than or equal to 0.05 were considered as statistically significant (*$p \leq 0.05$; **$p \leq 0.01$; ***$p \leq 0.001$).

In previous studies, membrane fluidity changes during carcinogenesis have been reported, proving the increase in membrane fluidity (Nakazawa *et al.* 1989; Zirong *et al.*, 1991; Ben-Bassat *et al.*, 1977). Increase in membrane fluidity has been linked with the cell transformation process. It has been thought that increase in membrane fluidity affects the tumor adhesion thus triggers the tumor metastasis. Zeisig *et al.* (2007) reported that, in breast cancer cells, domain organization of membrane directly affects the adhesive properties of tumor cells. In another study, membrane fluidity was inhibited via phosphodiesterase. It was observed that, cells with more flexible membrane structure could be able to join micro circulation easier (Ambrus *et al.* 1981).

As shown in Table 3-3, in carcinoma group the intensity of CH_3 stretching band is decreasing whereas that of CH_2 stretching band is increasing. This shows that the numerical ratio of methyl to methylene groups was decreased in malignant samples. However the absolute value of this decrease in ratio is not fixed in every patient.

3.1.1.1.3 Spectral analysis of 1700-1400 cm^{-1} region

Band located at 1452 cm^{-1} is overlapped with the band at 1462 cm^{-1} (band 6). The peak at 1462 cm^{-1} is regarded as a spectral point where the strong urea contribution exists. The possible reasons for the significant shifts in frequency to the higher points in carcinoma group might be the structural changes in the urea molecule or the decrease in number of Hydrogen bonding composing the urea structure. Urea is simple molecule and makes extensive hydrogen bonds with water. Urea-water interactions are so important for organisms thus it was investigated by several groups. However there is no clear understanding on the exact behavior of urea-water combination system. In the vibrational spectroscopy area, Hoccart and Turrell (1995) reported that the presence of more hydrogen bonds causes shifting of C-N asymmetric stretching vibrational frequency to the lower points that is supported also by our results.

Band 6 also overlaps with the CH_2 bending vibration of lipids (Cakmak *et al.*, 2003; Manorahan *et al.*, 1993). By interpreting the frequency of this band, it is possible to get information about the order state and interchain packing status of lipid bilayer. But for the study of membrane order properties mainly pressure dependence of this kind of vibrational mode has been used (Wong et al., 1990; Wong et al., 1993). Pressure dependence studies were not carried on this study instead C-H stretchings coming from lipid and proteins were taken into consideration. Thus the region between 3050-2800 cm^{-1} was evaluated with different perspective. In the 3050-2800 cm^{-1} range, observation of significant shift of band 6 in carcinoma group, make this band as a good candidate for bladder tumor detection.

The band located at 1628 cm^{-1} (band 5) is mainly corresponds to the C=O stretchings of amide I groups of structural proteins (Melin *et al.*, 2000; Takahashi *et al.*, 1991).

The intensity of this band is considerably increased in the carcinoma group (Table 3-3). This band is generally considered for the detection of protein content. Results showed increased protein content in carcinoma group. Possibly this might be sourced from the synthesis of cancer specific over expression of some glycoproteins and some other mulfunctional proteins. Over expression of glycoproteins were observed in many malignancies (Hochhauser *et al.*, 1991) and suggested as the way of gaining multidrug resistance of cancer cells (Gottesman *et al.*, 1996; Lum *et al.*, 1993). NMP22 and C7orf24 are two example proteins that have been used as markers for the detection of bladder tumor (Kageyama *et al.*, 2007). So targeted inhibition of some specific glycoproteins like P-gp, is investigated as a potential method for increasing the sensitivity of tumor cells to the drug therapy.

3.1.1.1.4 Spectral analysis of 1200-900 cm^{-1} region

Spectral region locating on 1200-900 cm^{-1} wavenumber, was shown as a major indicator of carcinogenesis (Chiriboga *et al.*, 1998; Wong *et al.*, 1991; Cohenford *et al.*, 1997). Indicated region gives valuable information about polysaccharides, phoshpholipids and nucleic acids. Therefore, many peaks within that region could be used as markers for tumor classification.

PO_2^- symmetric stretching band (band 7) at around 1076 cm^{-1} shifted significantly to the lower frequencies in carcinoma group (Table 3-2). Also the band area values of carcinoma samples increased significantly (Table 3-3). These kinds of changes in band intensities and peak positions were observed previously in many different cancers like basal cell carcinoma, colon, ovary, stomach and liver (Wong *et al.*, 1993; Rigas *et al.*, 1990; Wong *et al.*, 1990; Wong *et al.*, 1991). This band mainly originates from the phosphodiester backbone of nucleic acids. The possible contributions from the phosphate head groups of membrane lipids are regarded as negligible. So regarding our results it can be said that, in bladder tumors, hydrogen bonds in the phosphodiester groups increase.

Carbohydrate band (band 9) in the frequency of 1020 cm^{-1} is assigned to C-O bending of carboxyl groups in carbohydrate molecules. The frequency shifts (Table 3-2) and peak area (Table 3-3) values are significantly different between carcinoma and control groups ($p<0.05$*).
The possible reason for the increase in band area in tumor samples might be the same with the increase in the area of band 5. The cancerogenesis dependent over expression of glycoproteins might be resulted in the increase in both protein and carbohydrate content. Similar findings were previously reported by Liu et al. (2006). Frequency shift in this particular band can be attributable to change in saccharide composition and structural alterations in carbohydrates in cancerous cells. Mostly malignant cells have a tendency to produce abnormal carbohydrate chains like the increased branching structure of N-linked glycans (Orntoft *et al.*, 1999).

Peak located at around 927 cm^{-1} (band 10) is attributed to DNA (Dovbeshko et al., 2002). A considerable shift ($p<0.05$*) to the lower frequencies and significant increase in the band area ($p<0.05$*) were observed in carcinoma group (Table 3-2 & 3-3). During cancer progression, increase in nucleic acid concentration and changes in nucleic acid conformation have been documented (Wong *et al*, 1991; Wong *et al* 1993; Liu *et al.*, 2006). In tumorigenesis, primary alteration is the uncontrolled cell division and growth leading to significant change in nucleic acid content and conformation via abnormal induction of transcription and DNA replication mechanisms.

Additionally, ratio of nuclei/cytoplasm also increases during tumorigenesis (Sternberg *et al*, 1989). Frequency shifted to the lower values in carcinoma group which indicated an increase in existing hydrogen bond strength or the number of hydrogen bonding between DNA components (Rigas *et al.*, 1990; Wong *et al.*, 1991).

DNA stability is directly related with the hydrogen bonding level. Peak at 927 cm^{-1} specifically attributed to the left handed DNA (Z form), which is less stable than the regular B form DNA and has not been widely seen in organism. Rather it is more transient form mainly induced by some biological activity which later disappears. Aromatic amines are one of the major reasons for bladder tumor progression. Substitutions due to the aromatic amine exposure results in transversion mutations and it is thought that these mutations arise from base conversions in DNA backbone. This finally leads to the conformational alteration from B form to the Z form (Foster et al., 1983). Our results indicate that the area of band 9 and 11, that are also DNA bands, decreases in response to increase in band 10. So it can be suggested that formation of less stable Z form DNA is triggered by cancerogenesis.

3.1.2 Hierarchical Cluster Analysis

Due to the macromolecular analyses, ATR-FTIR spectra of control and carcinoma groups show significant differences. However, we encountered to some difficulties in the clustering of single individuals. In human studies, the variations within groups also exist considerably in addition to the variations between groups. Additionally, we used bladder wash sample as an examination material which can be affected from the diet of patient easily. So the number of sample to be investigated in grouping analysis is important. As it was stated before, there are considerably many candidate different spectral regions to conduct cluster analysis. We have observed the different regions to increase the discrimination success of study. Each selected region represents different macromolecular content of the sample. The best clustering of control and carcinoma groups were observed in the ranges of 1100-900 cm^{-1}, 900-832 cm^{-1}, 1500-1343 cm^{-1} and 2990-2820 cm^{-1}. Results are presented in the Figure 3-5, Figure 3-6, Figure 3-7 and Figure 3-8 respectively. For the first three regions, vector normalized second derivative spectra were used whereas non-processed spectra was preferred for the last region.

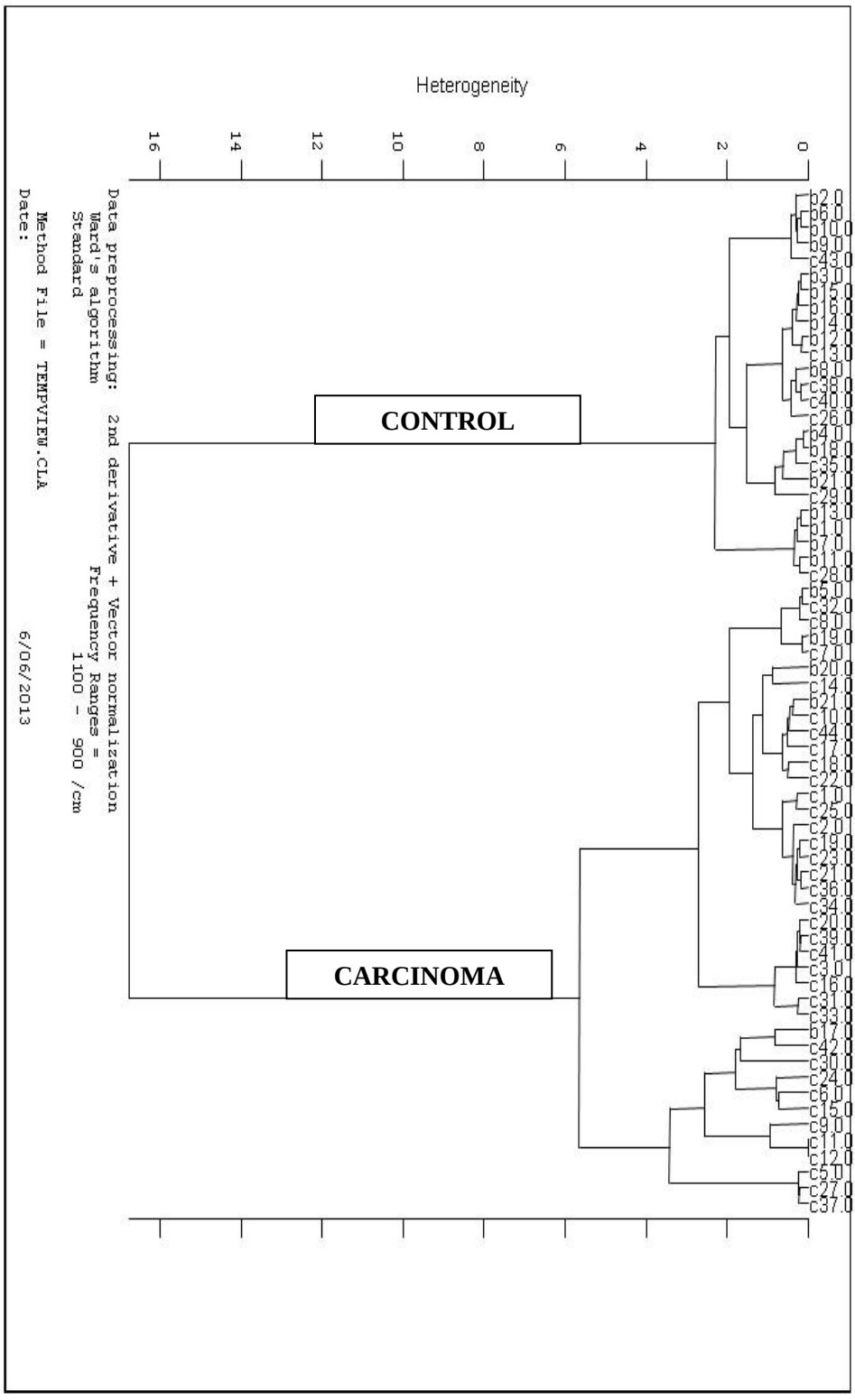

Figure 3-5 Hierarchical clustering of control and carcinoma samples using vector normalized second derivative spectra (spectral region: 1100-900 cm^{-1})

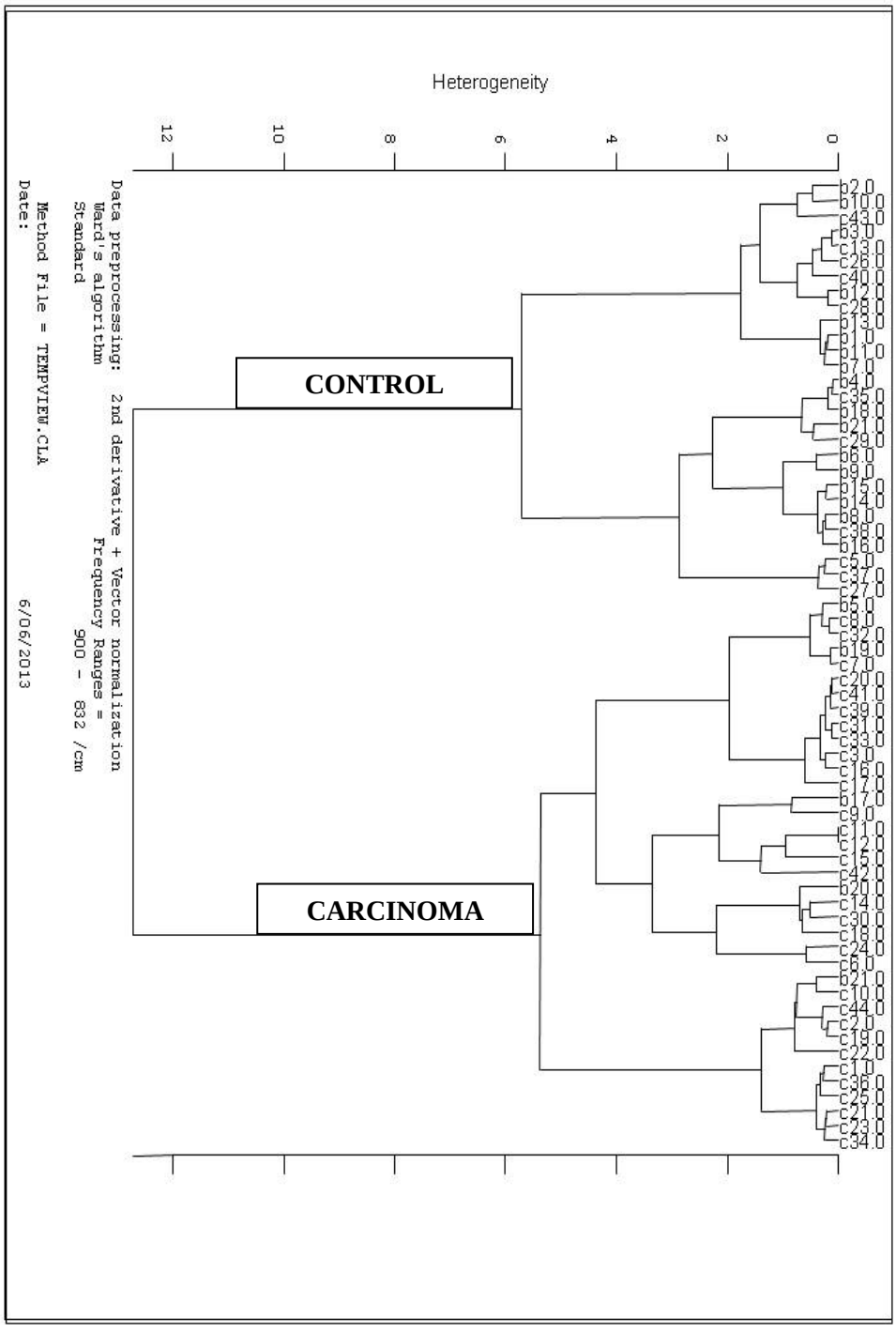

Figure 3-9 Hierarchical clustering of control and carcinoma samples using vector normalized second derivative spectra (spectral region: 900-832 cm^{-1})

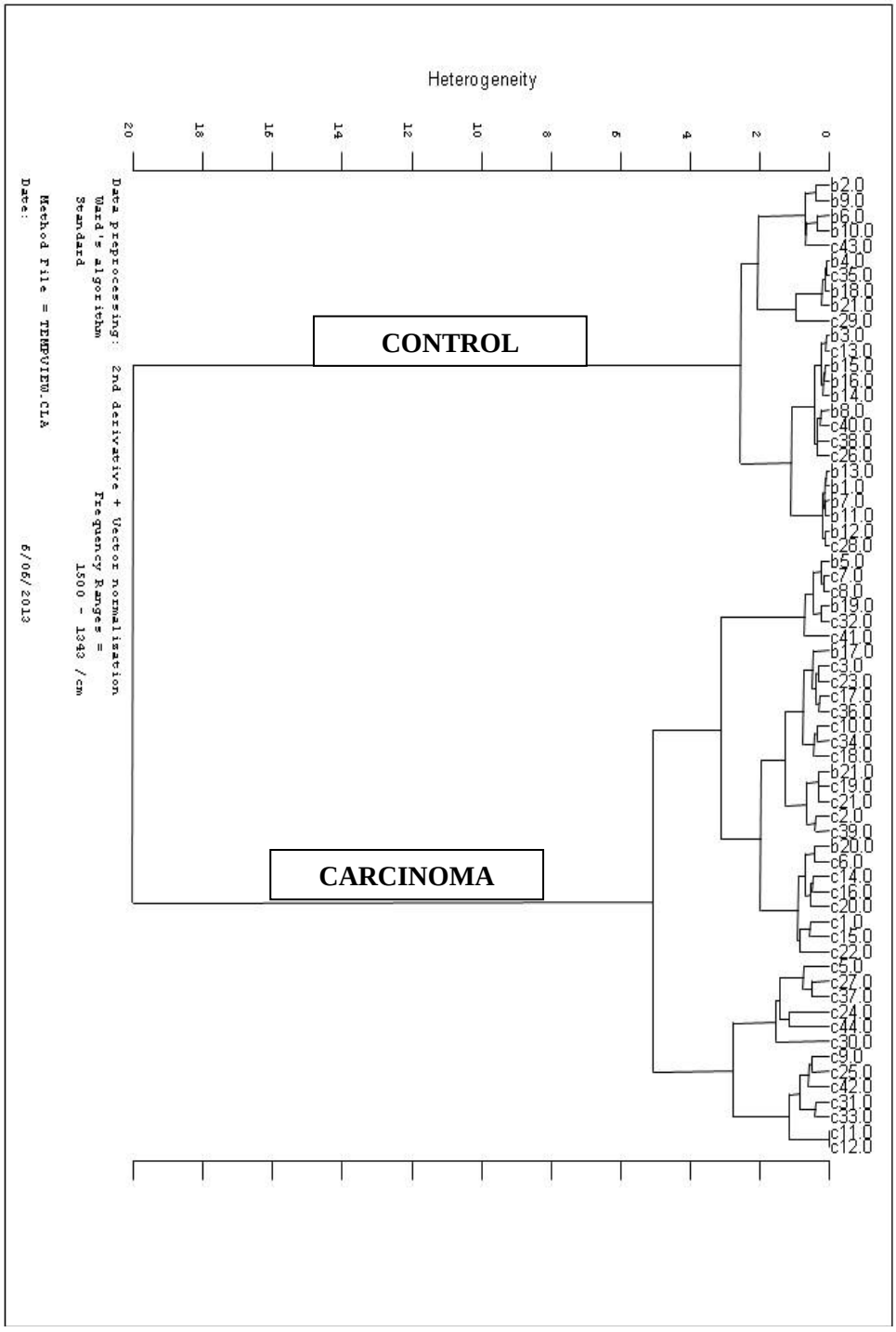

Figure 3-10 Hierarchical clustering of control and carcinoma samples using vector normalized second derivative spectra (spectral region: 1500-1343 cm^{-1})

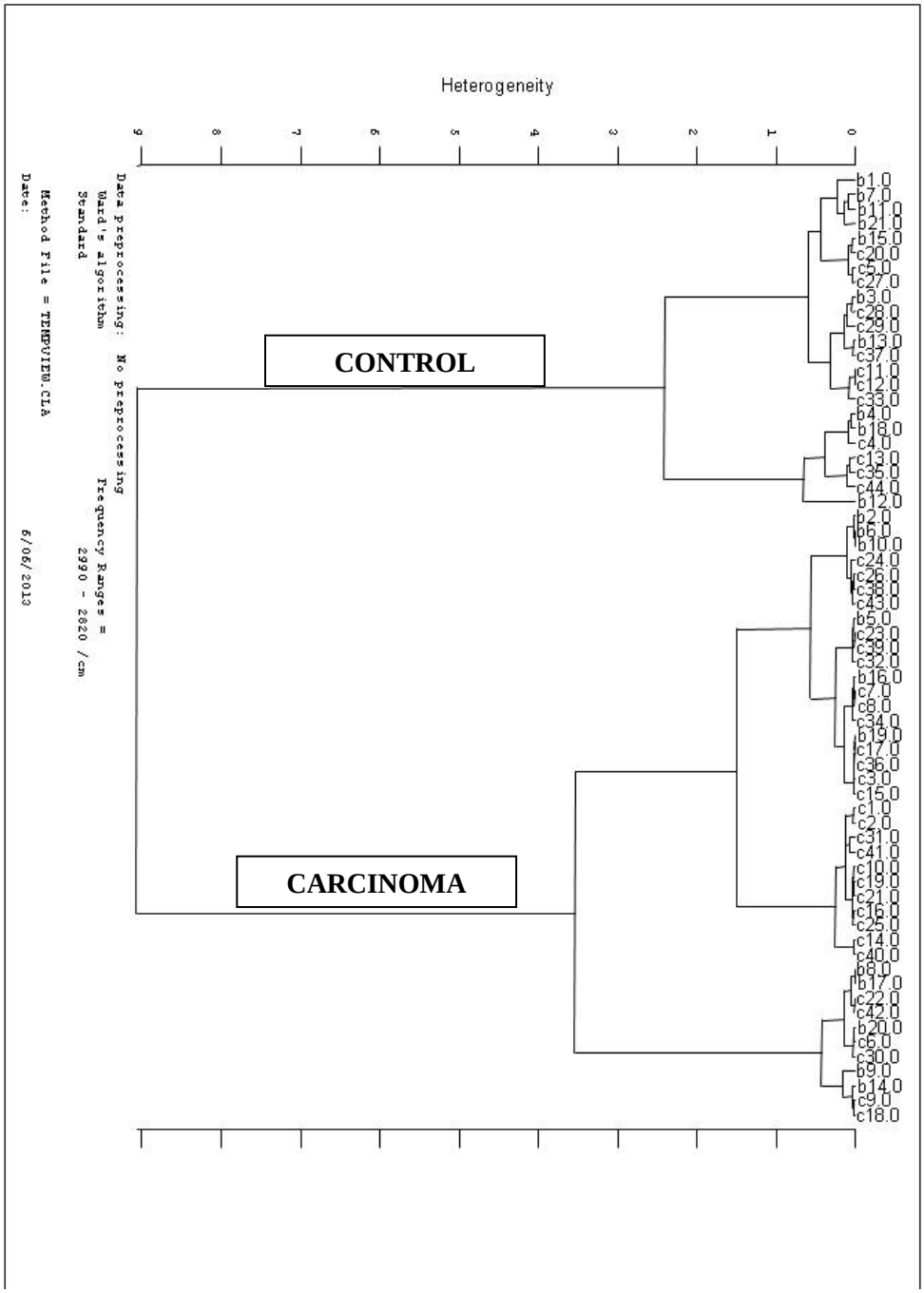

Figure 3-8 Hierarchical clustering of control and carcinoma samples using non-processed spectra (spectral region: 2990-2820 cm^{-1})

As it was indicated in the figures, we reached the highest sensitivity with the 92.5% and with 68% specificity in the 1100-900 cm^{-1} spectral region. Other sensitivity and specificity values were calculated as follows; 89.2% sensitivity and 60.7% specificity for 900-832 cm^{-1}; 90% sensitivity and 68% specificity for 1500-1343 cm^{-1} and lastly 73.8% sensitivity and 43.5% specificity for 2990-2820 cm^{-1} spectral range (Table 3-5).

Table 3-5 Sensitivity and Specificity values observed in different spectral regions

Spectral Ranges (cm^{-1})				
	900-832	**1100-900**	**1500-1343**	**2990-2820**
Sensitivity (%)	**89.2**	**92.5**	**90**	**73.8**
Specificity (%)	**60.7**	**68**	**68**	**43.5**

In our study, cytology sensitivity was determined as 45%. In the table below, the comparison of sensitivity and specificity values of commonly used bladder cancer diagnosis techniques is given. Values were shown as a range. The values can vary according to the grade and stage of cancer.

Table 3-6 Comparison of common bladder cancer diagnosis techniques (Adapted from Parker and Spiess, 2011)

Technique	Sensitivity (%)	Specificity (%)	Clinical Status
IMMUNOCYT	66.7 – 84.9	62 – 84.7	Laboratory
NMP 22	49.5 - 92	66 – 87.3	Laboratory
FISH	69 - 92	89 – 94.5	Laboratory
QUANTICYT	42 - 69	67.9 - 87	Investigational
HYALURONIC ACID (HA)	61 - 83	53.9 – 84.4	Investigational
MICROSATELLITE ANALYSIS	60 - 97	93	Investigational
BTA stat	67 - 70	75 - 78	Investigational
CYTOLOGY	12.2 - 79	78.4 – 96	Laboratory

The overall sensitivity of our method in three spectral regions, are much higher than the urine cytology which have been accepted as universal bladder cancer diagnosis technique. Additionally ATR-FTIR technique provides much quicker and more cost-effective analysis opportunity than cytology. More importantly, it serves as a computational, automated technique which has not been dependent on the subjective evaluation of pathologist. Also, FTIR spectroscopy can detect minute changes and give molecular information due to the cancerogenesis. Collected information can be used as an input data for much earlier diagnosis than the other conventional techniques. As an example case, FTIR spectroscopy was previously used for the determination of diabetes induced changes in very early phases by our group (Toyran *et al.*, 2006).

When we compared our results with the overall specificities and sensitivities of other common cell or urine based techniques (Table 3-6), we could reach higher sensitivity than all of these techniques in the spectral regions of 1100-900 cm^{-1}, 900-832 cm^{-1} and 1500-1343 cm^{-1}. Also the overall specificity of ATR-FTIR was observed to be higher than some of these techniques including BTA stat, Quanticyt and NMP22 in the 1100-900 cm^{-1} and 1500-1343 cm^{-1} range. In this study, analyzed patient number was limited. We believed that, both the sensitivity and specificity values would be increased with the increase in number of patients. The other possible reason of low specificity of our technique might be the early diagnosis ability of the FTIR spectroscopy which may diagnose the disease at a very early stage. Healthy patients, classified in diseased group may develop bladder tumor in near future.

3.2 Study II: Botanical Origin Estimation of Turkish Honey Samples

ATR-FTIR spectroscopy has been used to study the honey samples to compare the spectral differences among them in the 4000-650 cm^{-1} region. General representational ATR-FTIR spectrum of a honey is given in Figure 3-9 and the general band assignment for important characteristic regions adapted from the previous studies in relevance is shown in Table 3-7.

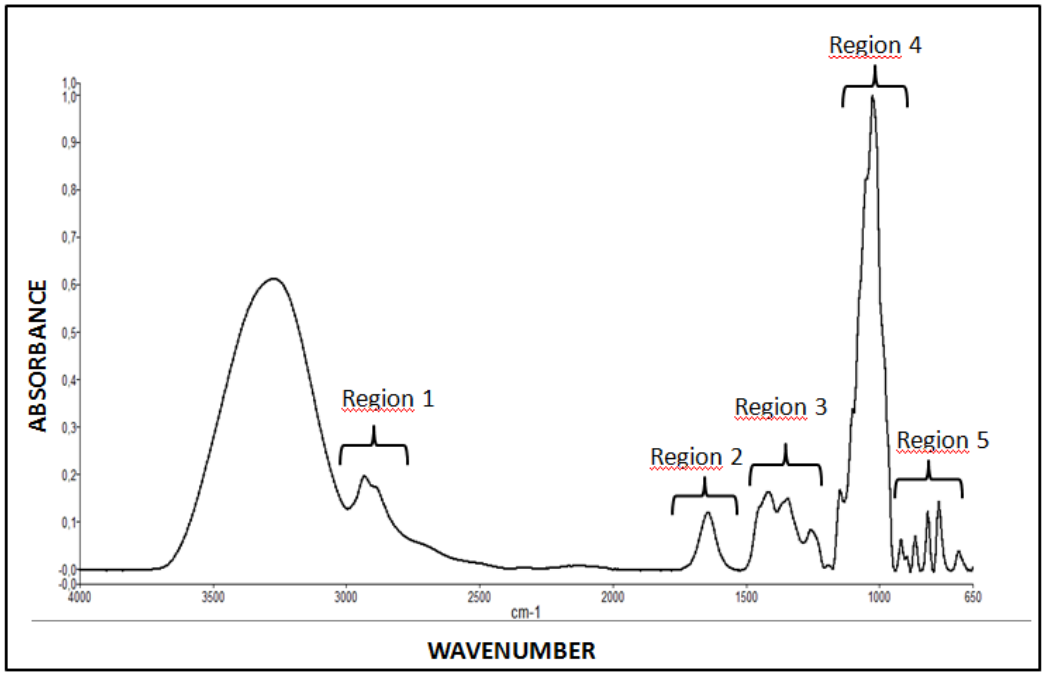

Figure 3-9 Representative ATR-FTIR spectrum of honey in the 4000-650 cm^{-1} spectral region

Table 3-7 Positions of honey characteristic bands

Region 1	3000-2800 cm^{-1}	**C-H stretching (carbohydrate)** **O-H stretching (carboxylic acids)** **NH_3 stretching (free aminoacids)**
Region 2	1700-1600 cm^{-1}	**C = O stretching** **C - N stretching** **N – H bending of Amide I (mainly proteins)**
Region 3	1540-1175 cm^{-1}	**N-H bending** **C-N stretching of Amide III (mainly proteins)** **CH_2 wagging (Carbohydrates)**
Region 4	1175-940 cm^{-1}	**C=O stretching of ketones** **C-O stretching** **Ring vibrations (mainly from carbohydrates)**
Region 5	940-700 cm^{-1}	**C-H bending** **Ring vibrations (mainly from carbohydrates)**

3.2.1 Molecular Characterization of Honey Spectrum

The region, between 1500-750 cm^{-1}, indicates the absorption bands of mono and disaccharides including, glucose, sucrose and fructose. The spectral region located between 900-750 cm^{-1}, also signify the anomeric region which is the characteristic structural component of saccharide conformation (Tul'chinsky et al., 1976). The bands located in the region of 900- 1150 cm^{-1} correspond to the stretching of C-O and C-C bonds whereas the ones located on the spectral region of 1200-1475 cm^{-1} are sourced from the O-C-H, C-O-H and C-C-H bendings (Hineno, 1977). The NH_3 stretching observed in the 3100-2600 cm^{-1} spectral region, especially the peak at around 2930 cm^{-1}, most probably originated due to the primary aminoacids that contribute to the honey composition with low concentrations (Chen and Irudayaraj, 1998). The peak present around 1415 cm^{-1} denotes the CH=C bond of fumaric acid (Weston et al., 2000). Thus the region between 1200-800 cm^{-1} could be regarded as carbohydrate region while the organic acids and amino acids absorptions are assigned to 3200-2800 and 1800-1200 cm^{-1} spectral regions.

The band frequency and band area values of 12 selected bands from different regions are shown in table 3-8 and 3-9 respectively.

Table 3-8 The band frequency values for all groups. The values are denoted as Mean ± Standard deviation. Significance degree was shown as *** for $p < 0.001$

	Frequency							
Band	Flower (n=36)	Tree (n=33)	Rhododendron (n=30)	Maple Syrup (n=3)	Fructose (n=3)	Grape molasses (n=3)	Adultered (n=3)	P value*
1	2931.69±0.37	2931.95± 1.26	2931.98±0.01	2932.75±0.008	2934.33± 0.002	2935.67±0.006	2934.11± 0.001	0.001***
2	2889.35±0.11	2889.64± 0.38	2889.26±0.003	2890.77±0.002	2889.55± 0.002	2890.32±0.003	2889.46± 0.002	0.001***
3	1642.43±0.29	1641.67± 0.69	1642.23±0.007	1641.08±0.01	1642,3± 0.002	1639±0.002	1640,62± 0.01	0.001***
4	1413.85±0.39	1413.34± 0.46	1413.75±0.02	1417.02±0.006	1414.35± 0.007	1411.43±0.006	1413.04± 0.009	0.001***
5	1344.1±0.32	1344.21± 0.26	1344.13±0.01	1362.13±0.03	1343.45± 0.001	1345.02±0.003	1343.46± 0.005	0.001***
6	1249.95±0.12	1250.5± 0.93	1250.09±0.01	1260.65±0.001	1249.88± 0.004	1251.52±0.003	1250.22± 0.005	0.001***
7	1048.67±0.32	1049.09± 1.29	1049.04±0.03	1048.09±0.002	1050.05± 0.012	1052.74±0.014	1049.27± 0.003	0.001***
8	1023.83±1.18	1024.04± 2.58	1024.93±0.04	1026.62±0.009	1026.7± 0.001	1028.85±0.008	1025.98± 0.006	0.001***
9	917.85±0.19	918.3±1.17	918.078±0.003	991.37±0.04	918.19± 0.003	916.74±0.004	918.61± 0.003	0.001***
10	864.55±0.05	864.56± 0.38	864.79±0.01	856.1±0.22	864.71± 0.002	863.8±0.005	864.89± 0.003	0.001***
11	816.76±0.08	816.88± 0.09	816.87±0.01	810.75±0.02	816.71± 0.001	816.09±0.004	816.69± 0.001	0.001***
12	775.08±0.15	775.08± 0.55	775.39±0.01	766.53±0.004	775.57± 0.007	773.31±0.01	775.48±0.0 04	0.001***

Table 3-9: The band area values for all groups. The values are denoted as Mean ± Standard deviation. Significance degree was shown as *** for p<0.001

	Band Area							
Band	Flower (n=36)	Tree (n=33)	Rhododendron (n=30)	Maple Syrup (n=3)	Fructose (n=3)	Grape molasses(n=3)	Adultered (n=3)	P value*
1	1.67±0.07	1.59±0.1	1.69±0.04	1.11±0.008	1.35±0.01	0.71±0.02	1.36±0.008	0.001***
2	1.44±0.1	1.26±0.14	1.47±0.04	0.71±0.01	0.9±0.009	0.37±0.01	0.91±0.004	0.001***
3	4.25±0.17	5.03±0.46	4.48±0.08	6.75±0.05	5.15±0.02	7.51±0.01	5.7±0.03	0.001***
4	1.99±0.03	1.99±0.19	2.24±0.04	10.1±0.07	3.72±0.06	16.14±0.11	1.93±0.008	0.001***
5	1.16±0.03	1.09±0.1	1.19±0.01	4.94±0.04	0.97±0.009	4.77±0.02	0.92±0.001	0.001***
6	0.87±0.03	0.92±0.09	0.9±0.02	3.59±0.03	1.07±0.005	0.79±0.008	0.98±0.005	0.001***
7	13.69±0.17	13.25±0.7	13.67±0.21	12.52±0.1	1.73±0.005	1.28±0.005	12.48±0.04	0.001***
8	24.84±0.53	23.91±1.63	24.83±0.26	1.49±0.005	13.11±0.04	4.11±0.01	19.86±0.05	0.001***
9	0.61±0.02	0.46±0.05	0.25±0.01	0.46±0.009	0.14±0.005	0.16±0	0.5±0.004	0.001***
10	0.61±0.02	0.57±0.04	0.62±0.01	0.26±0.004	0.61±0.005	0.37±0.02	0.61±0.004	0.001***
11	1.03±0.03	0.9±0.09	1.01±0.01	0.3±0.009	1.03±0.005	0.65±0.005	1±0.005	0.001***
12	1.58±0.04	1.45±0.04	1.58±0.02	10.04±0.12	1.42±0.009	1.01±0.005	1.37±0.005	0.001***

3.2.2 Molecular Investigations

The most significant differences were realized between 1600 and 800 cm^{-1}. Especially the regions between 1050 and 950 cm^{-1} representing the C-O and C-C stretchings of carbohydrate chains, causes main variations within sample groups (Figure 3-10 and enlargement A), supporting to the previous studies.

In absorption spectroscopy, if the measured amount of sample and the thickness of sample are same, the band area values give the relative concentrations of functional groups that are assigned to the band of interest.

3.2.2.1 Spectral Analysis within Protein Bands

The absorption of amide I band is mainly related with the C=O stretching of amide molecules in protein structure. The frequency values of amide I changing depending on the differences in protein conformation so it can be used for the protein secondary structure determination (Liu et al., 1996; Severcan & Haris, 2003). In the current study, (Figure 3-11), relative significancies of amide I frequency values of all groups due to the adultered honey were calculated. Results revealed that the protein secondary structures show significant differences among all sample groups.

When the comparison of Amide I band intensity values is considered, a significant increase was observed in non-honey samples (grape molasses, maple syrup and fructose syrup). However water molecules give strong absorption between 1640 and 1650 cm^{-1} (Cai and Singh, 2004). As priory knowledge, fructose syrup sample has not protein contribution. From those results, it can be inferred that, increase in the amide I band intensity is sourced from the water contribution rather than protein molecules. The amount of water is much more in non-honey samples as compared to natural honeys.

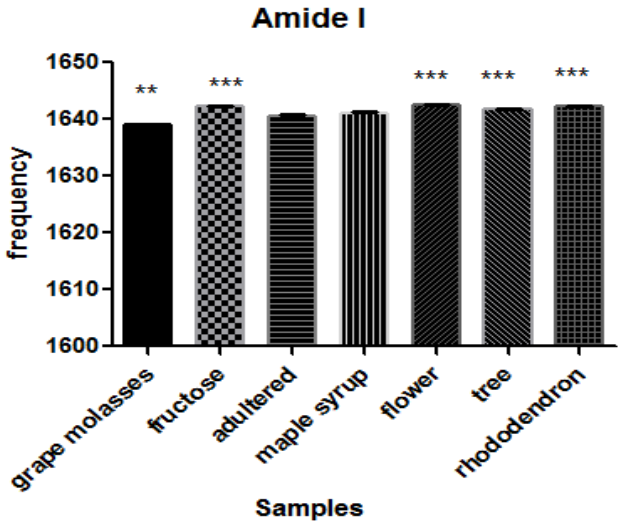

Figure 3-11 Comparison of band frequency values of Amide I band among all groups

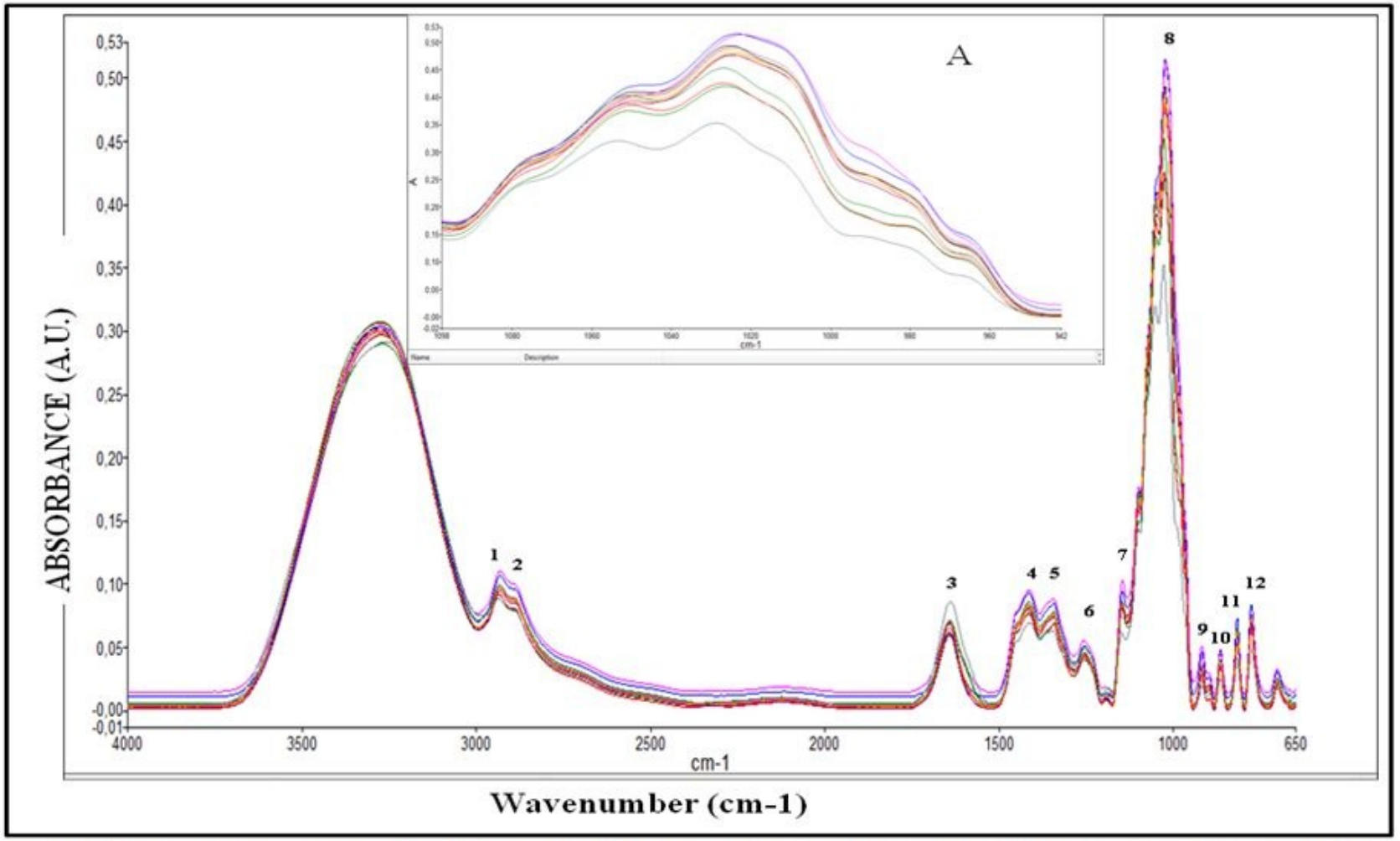

Figure 3-10 ATR-FTIR spectrum of all sample groups in 4000-650 cm^{-1} and the Enlargement (A) of the spectral region between 1100-950 cm^{-1}

The 3rd region observed within 1540-1175 cm^{-1} is assigned as amide III corresponding to N-H vibrations. Amide III also informative about the α-helix between 1280-1320 cm^{-1}, β-turns at 1254-1280cm^{-1}, β-sheets at 1230-1245 cm^{-1} and random coils within 1250-1260 cm^{-1} ranges. To detect this changes quantitively, vector normalized, 2nd derivative spectra can be used. Changed sub-band area values give information about the corresponding secondary structure pattern (Tantipolphan et al., 2008). Amide vibrations are influenced by, amino acid side chain absorptions, dielectric specificities of solvent and additionally the steric situation of molecules (Dousseau and Pezolet, 1990). Amide III bands have less water contribution then the amide I and represent more complex nature than amide I. At around 1340 cm^{-1}, CH_2 wagging vibrations of carbohydrate molecules contribute to the band 5. On the other hand band 6 mainly composed of amide III vibrations of proteins. To eliminate the effect of vibrational contributions coming from carbohydrates, the ratio of band 5 to band 6 was used for the evaluation of protein intensity in samples.

As it can be seen in histogram (Figure 3-12) dramatic shift to higher values was observed for frequency of amide III vibration (band 5), in grape molasses and maple syrup due to the adultered honey. However although the shifting are small for the remaining groups, they were significant according to Tukey test.

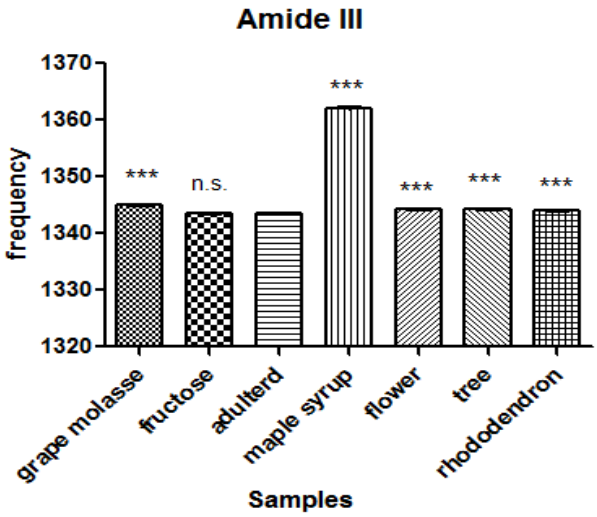

Figure 3-12 Comparison of band frequency values of Amide III band among all groups

Figure 3-13 indicates that the protein level is much higher in honey samples than adultered honey and fructose syrup as expected. Maple syrup has nearly same amount of protein with honey samples. However grape molasses include relatively the highest protein content among all.

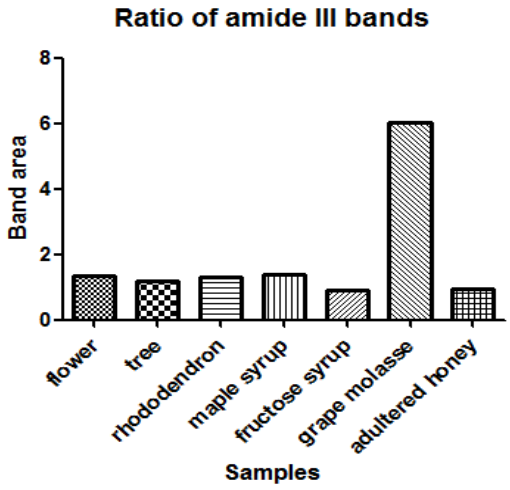

Figure 3-13 Comparison of band area ratios of band 5 / band 6 among all groups

3.2.2.2 Spectral Analysis within Carbohydrate Bands

The region located between 1175-700 cm^{-1} expresses the various kinds of carbohydrate vibrations. In a given representative spectrum in Figure 3-14, frequency shifts and band intensity differences among all groups can easily be observed.

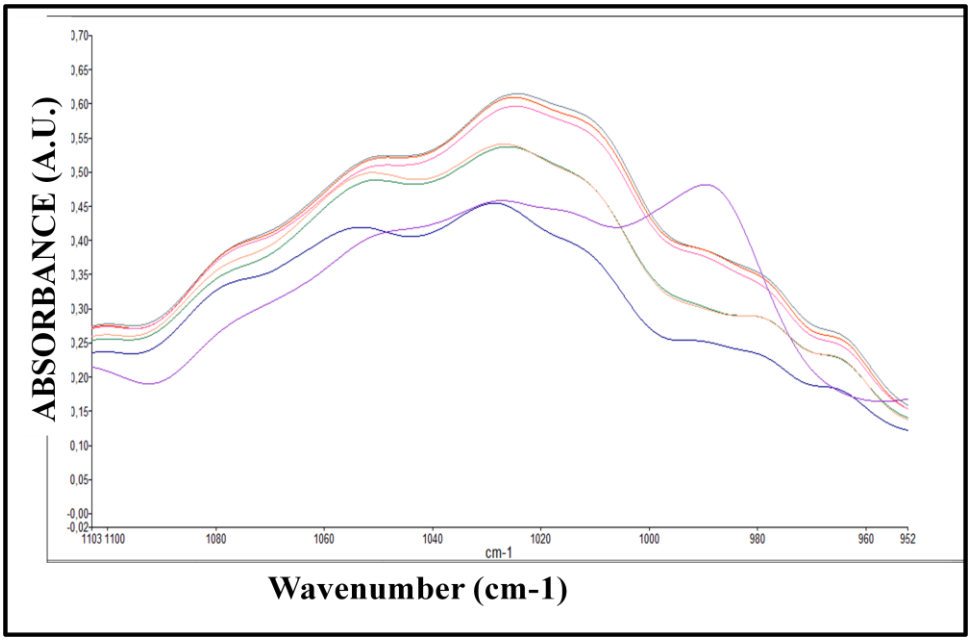

Figure 3-14 Comparison of sample groups within 1100-950 cm^{-1} spectral region

Bands, presented between the indicated interval, were evaluated in terms of band area values to get clues about the carbohydrate concentrations (Figure 3-15).

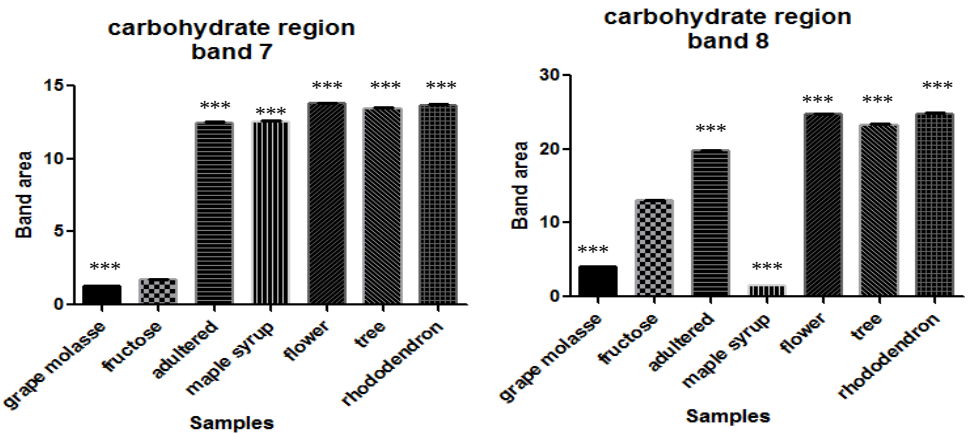

Figure 3-15 Comparison of band area values among all groups within 1100-950 cm^{-1} spectral region. One way ANOVA with Tukey post-hoc test was used for statistical analysis. (***) represents the significancy compared to fructose group. The *p* values less than or equal to 0.05 were considered as statistically significant (***$p \leq 0.001$).

As can be seen in Figure 3-15, in band 7 and 8 fructose concentration was lower in our fructose syrup sample. Significancy values of each group compared to fructose syrup were calculated and founded as; $p<0.001$ (***).

Also we know that maple syrup is rich in glucose rather than other carbohydrates. For bands 9, 10 and 11, significancy values compared to maple syrup were calculated as $p\leq0.001$ (***) for each sample group. This indicates that the band 7 and 9 can be assigned as mainly glucose dominant band whereas bands 8, 10 and 11 could be regarded as fructose dominant ones (Figure 3-17).

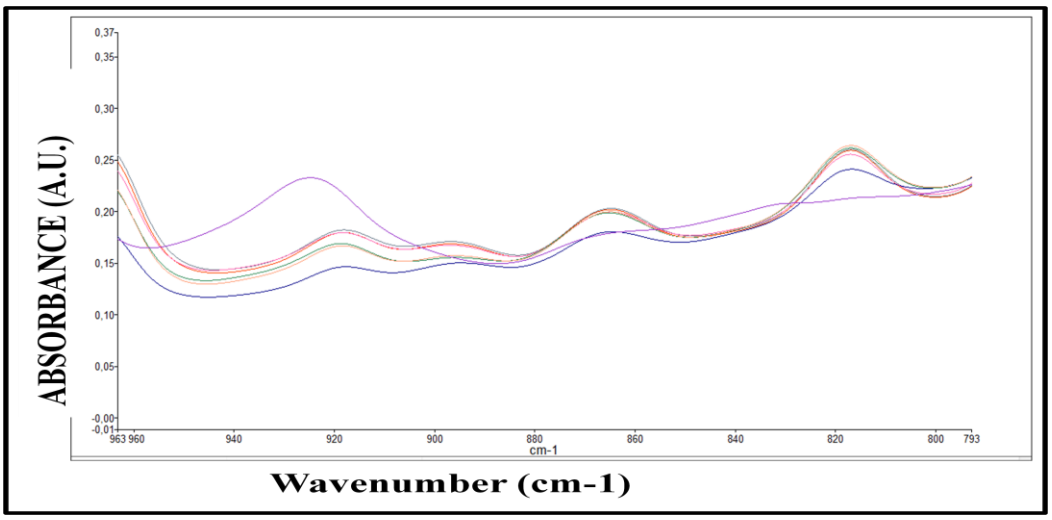

Figure 3-16 Comparison of sample groups within 950-790 cm^{-1} spectral region

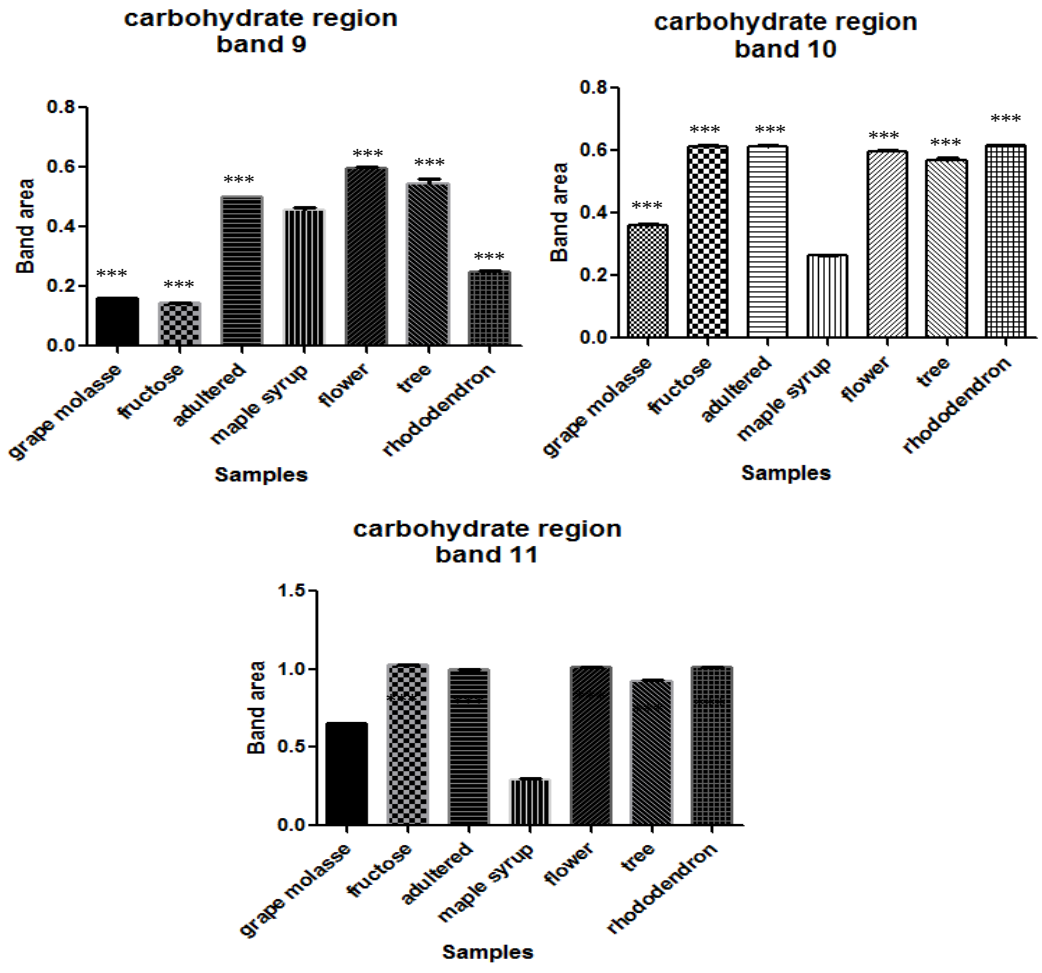

Figure 3-17 Comparison of band area values among all groups within 950-790 cm^{-1} spectral region. One way ANOVA with Tukey post-hoc test was used for statistical analysis. (***) represents the significancy compared to fructose group. The *p* values less than or equal to 0.05 were considered as statistically significant (***$p \leq 0.001$).

In this study, the characteristic ATR-FTIR spectrum of grape molasses and different honey types were firstly compared. Spectrum of molasses was observed and compared with the average spectrums of different honey types and searched for differences due to the Vitamin A, Vitamin B1 (thiamine), Vitamin B2 (riboflavin) and also niacin content.

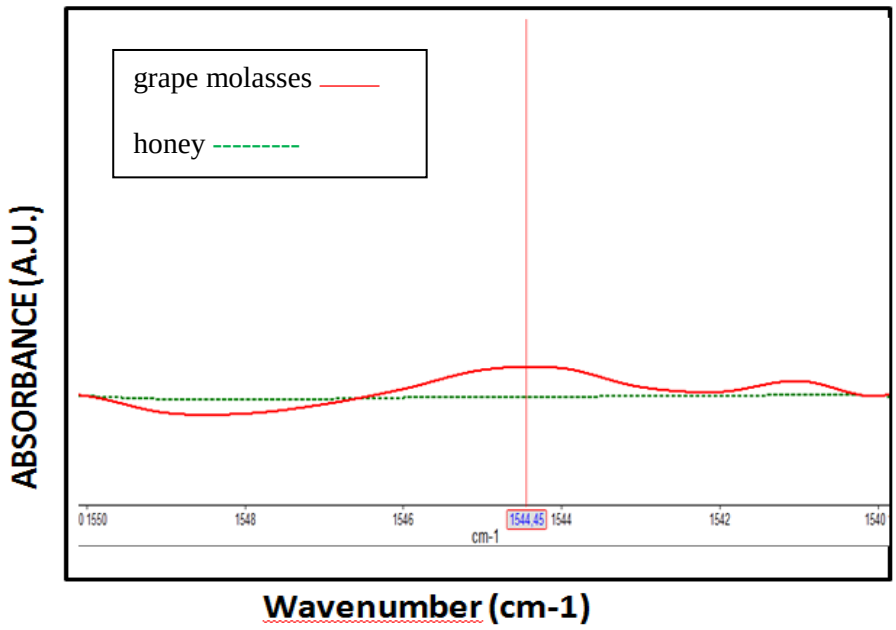

Figure 3-18 Comparison of peak at 1544 cm^{-1} in honey and grape molasses samples

In figure 3-18, difference between grape molasses and average honey spectrum in terms of Vitamin B1 content, was shown. In literature the frequency value where the thiamine molecule gives a peak, was stated as 1544 cm^{-1} (Wojciechowski et al., 1997). A distinct peak was observed at 1544 cm^{-1} in molasses spectrum. It can be clearly said that grape molasses contain much more thiamine molecule than honey. For other vitamin types, there were no observable differences between grape molasses and honey.

3.2.3 Categorization of Investigated Honey Samples Based on their Amino acid and Carbohydrate Patterns

Chemometric classification methods for the determination of botanical origin were applied in defined different ranges. As mentioned earlier, spectral regions between 3200-2200 and 1500-950 cm^{-1} correspond to organic and amino acids, carbohydrates, and vitamins that are more specifically represent glucose, fructose, sucrose, fumaric acid, lactic acid, malic acid, succinic acid, gluconic, acid, citric, acid, riboflavin, ascorbic acid (Vit. C), thiamin (Vit B1), pyridoxine (Vit B6), niacin, acetylcholine, L-cystein and dimethylxanthine.

3.2.3.1 Principal Component Analysis

A mean-centered Principal Component Analysis was conducted on the ATR spectra over the range of 4000-650 cm^{-1} (Figure 3-19) & 1700-1600 cm^{-1} (Figure 3-20). Distinct segregation and clustering between the samples are apparent in both figures.

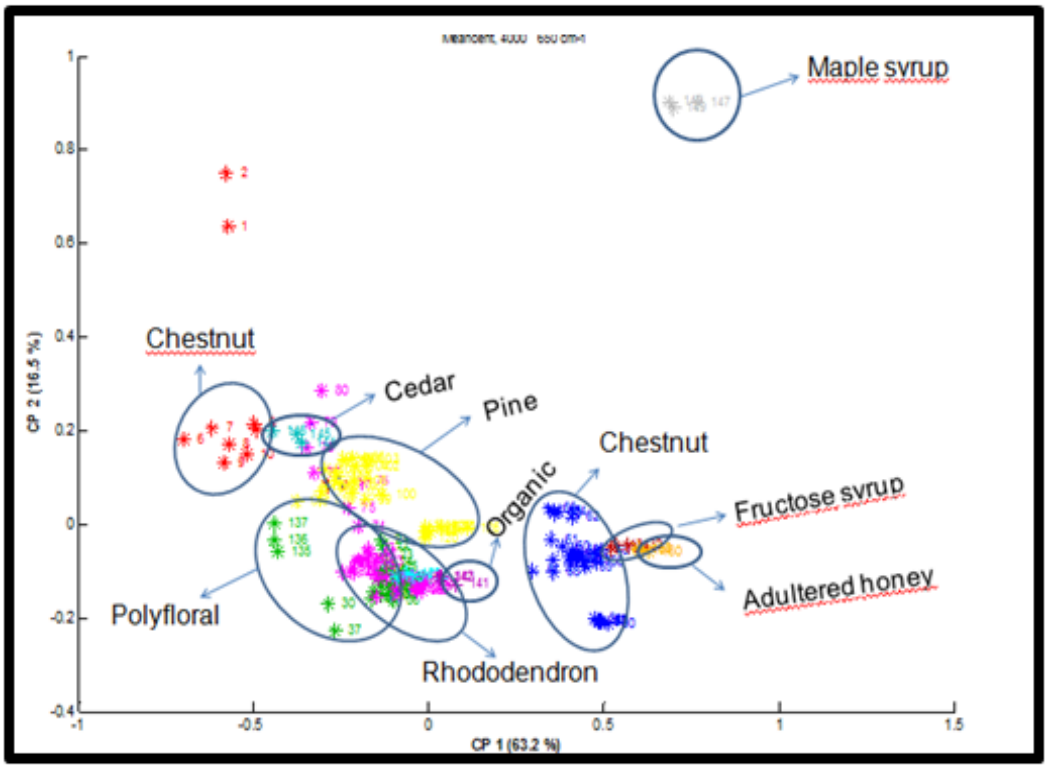

Figure 3-19 PCA scatter plot of all honey samples over the 4000-650 cm^{-1} spectral region

Samples were grouped close together, creating uniform clusters for each of the analyzed honey types in the PCA scatter plot. PCA was applied to whole group of FTIR spectra, obtaining an evident discrimination (score plot) of the different pure honey samples with respect to the adulterated honey (Figure 3-19). Although it is very hard to see discrimination over whole spectra in biological samples, here highly successful significant differentiation of all investigated groups has been achieved. Only rhododendron samples make penetrations to both tree and flower originated groups. This result in consisted with what we expected, as the rhododendron itself classified as briar patch, it can give close results both tree and flower originated samples.

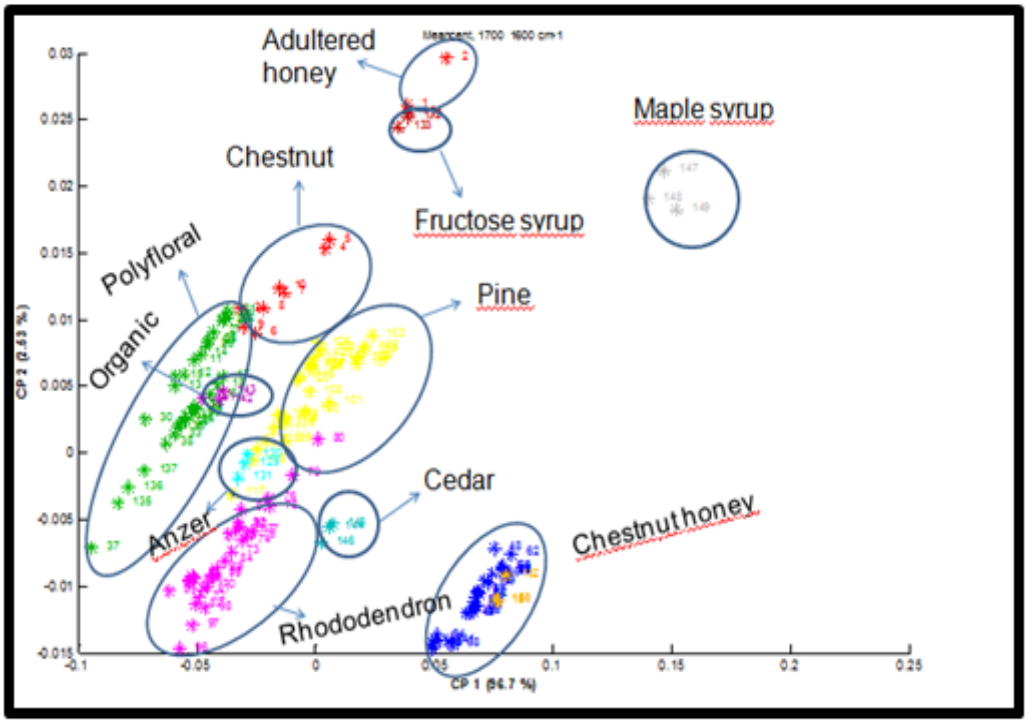

Figure 3-20 PCA scatter plot of all honey samples over the 1700-1600 cm^{-1} spectral region

It can be observed a clear splitting of the data as depicted by the first two principal components in the Amide I region with the values of 96.7% for CP1 and 2.53% for CP2 (Figure 3-20). The band at 1640 cm^{-1} (amide I) accounts for the C=O (70-85%) and C–N stretching modes of vibrations (10-20%). Results confirmed that the groups significantly differ in terms of protein concentrations and structure from each other. Especially non-honey samples like maple and fructose syrup in addition to adultered honey were grouped considerably far away from the rest. Classification pattern of the samples with PCA are in consisted with the results of hierarchical clustering.

3.2.3.2 Hierarchical Clustering Analysis

The anameric region at 950-750 cm^{-1} was frequently preferred for the spectral analysis of carbohydrates in IR spectroscopy. Analysis in this range make possible to distinguish bands characteristic for α and β conformers or pyranoid and furanoid ring vibrations of mono and polysaccharides (Mathlouthi & Koenig, 1986). Therefore, 1800-750 cm^{-1} spectral region where mainly the carbohydrate specific ring vibrations are resided, was selected for successful discrimination of clusters.

For the calculation of sample similarities, the Euclidean distance was used indicating the complete linkage clustering values. The results obtained are represented in Figure 3-21 in the form of dendrograms.

Clear cut classes were gathered over the range of 1800-750 cm^{-1} with high heterogeneity values (up to 5). All of the tree originated samples (chestnut, cedar, pine) are aggregated in one cluster on the left arm. As the maple syrup is also the maple tree originated sample, it shows more similarity to tree originated group than to the flower originated ones.

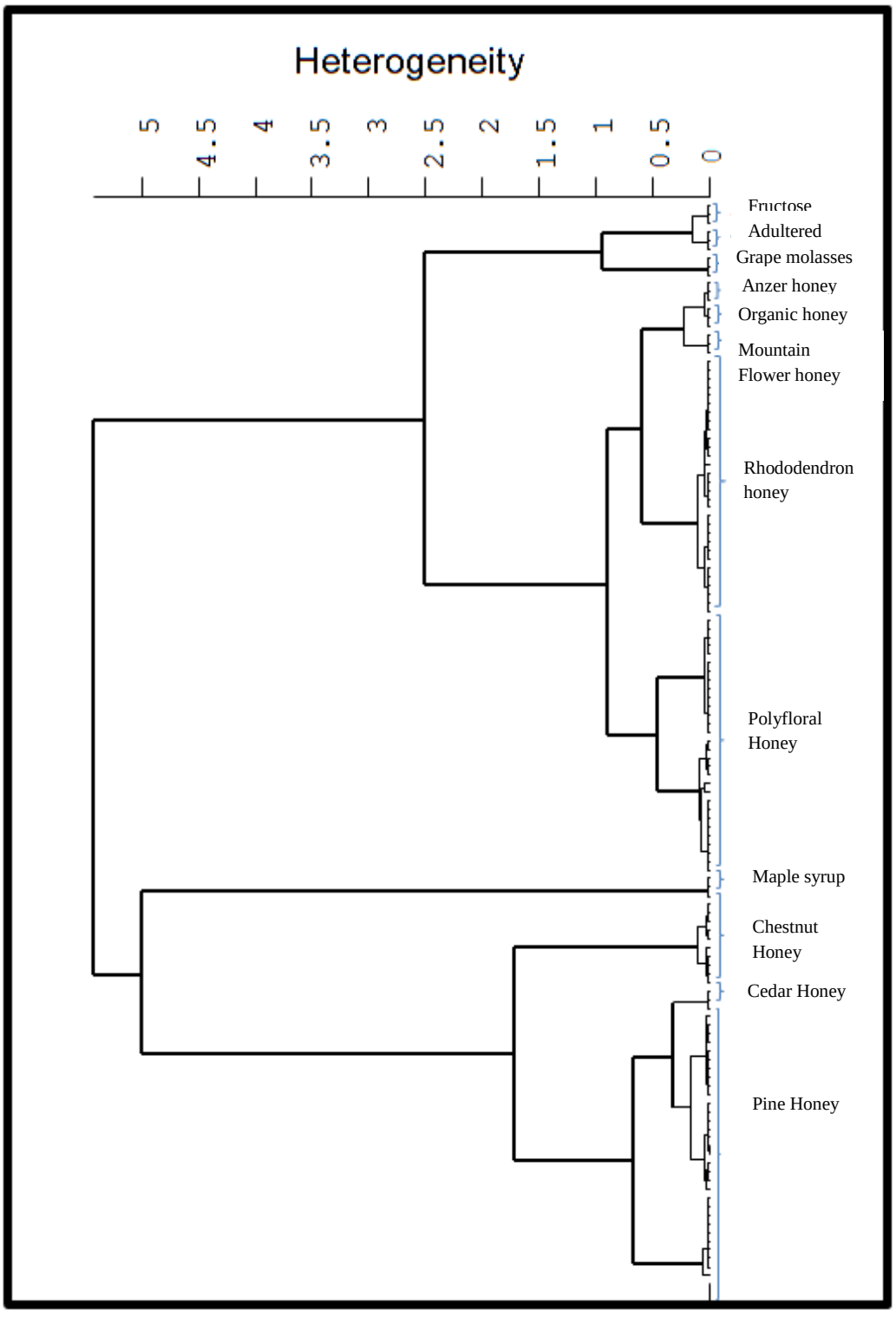

Figure 3-21 Hierarchical Clustering of all samples

One arm of the second cluster is composed of flower originated honey samples including polyfloral, anzer, organic, mountain flower and rhododendron honeys. Anzer, organic and mountain flower honeys are region specific samples, it is known that the purity of their botanical origins is higher than polyfloral honey group. So they were clustered in the same arm. As the rhododendron honey is collected from the mountains, it was clustered closer to that group than polyfloral ones. Fructose syrup, grape molasses and the adultered honey were agglomerated on the far right arm of the second cluster in that they differ from the natural samples in terms of their carbohydrate content significantly.

A 100% correct classification was achieved in the indicated spectral region with cluster analysis.

CHAPTER 4

CONCLUSION

With the help of infrared spectroscopy, biomolecules can be observed in a single experiment by decoding all infrared vibrational modes of all molecules as a mixture that composed of the sample of interest. Thus many of the spectral features are superimposed. So most of the time it is impossible to gather information about single specific compound, from tissues, biological fluids or cells. Rather the infrared spectra implement spectroscopic fingerprints of total biochemical composition of the sample of interest. In an infrared spectrum, characteristic absorption signals coming from proteins, lipids, carbohydrates, nucleic acids and other molecular compounds are monitored simultaneously via encoding a huge amount of information which has significant biodiagnostic potential.

Bladder cancer therapy spans long term, including tumor therapy and follow-up period. Especially frequent long-term follow-up raises the costs spent on. A commonly preferred gold standard technique in Clinique, cystoscopy, notably disturbs the patient comfort because of its invasiveness. Another important problem, the subjectivity of biopsy interpretations, leads to inconsistencies. A new, less costly, objective and automated approach in diagnosis and screening of bladder tumor is needed. In this current study, we aimed to introduce ATR-FTIR spectroscopy as a method for bladder cancer diagnosis from bladder wash samples. It is the first time that the bladder wash sample has been used for bladder cancer diagnosis by ATR-FTIR spectroscopy. The constituent of bladder wash sample is so similar to voided urine which may open up a way to diagnose urogenital cancers directly from urine in the near future.

Results demonstrated that ATR-FTIR could be used to detect cancerous tumor development from bladder wash sample with better sensitivity and specificity than urine cytology. Advantageously, ATR-FTIR gives results in much shorter time than all of the currently used methods. Additionally, technique provides opportunity to get results in a much less costly manner. When the number of sample belonging to each grade of bladder cancer have been increased, it would be possible not only detect the presence of tumor but also to classify tumor in terms of their grade with higher sensitivity and specificity. On the other hand the use of ATR-FTIR has been shed light on the bladder cancer development by deciphering the changes in macromolecular level in the spectral fingerprint regions.

In the second part of the thesis study, estimation of botanical origins of seven different Turkish honeys was confirmed with ATR-FTIR spectroscopy. Gathered results from the

botanical origin estimation of honey study pointed out that, there are many considerable variations in the spectral parameters of honey samples coming from different botanical origins. Especially the variations in the protein and carbohydrates dominantly determine the specific spectral pattern of each sample. Results further revealed that physicochemical differences provide enough information for the differentiation of honey samples originating from different botanical origins. ATR-FTIR spectroscopy in combination with multivariate analysis enables to pick up of the number of quantitative information via single rapid measurement for honey botanical origin classifications. Based on spectral variations, differentiation with the highest specificity and sensitivity values was obtained with hierarchical clustering analysis. Results of this study exposed the potential power of ATR-FTIR spectroscopy in automated and highly sensitive botanical origin estimation of honey.

REFERENCES

- Alissandrakis, E.; Daferera, D.; Tarantilis, P. A.; Polissiou, M.; Harizanis, P. C. (2003). Ultrasound-assisted extraction of volatile compounds from citrus flowers and citrus honey. Food Chem. 82, 575-582.

- Amling, C.L. (2001). Diagnosis and management of superficial bladder cancer. Curr. Probl. Cancer. 25: 219–78.

- Ampuero, S.; Bogdanov, S.; Bosset, J. O. (2004). Classification of unifloral honeys with an MS-based electronic nose using different sampling modes: SHS, SPME, and INDEX. Eur. Food Res. Technol. 218, 198-207.

- Andrus, P. G. (2006). Cancer monitoring by FTIR spectroscopy. Technology in Cancer Research and Treatment. 5(2), 157–167.

- Andrus, P. G. L., and Strickland, R. D. (1998). Cancer grading by Fourier transform infrared spectroscopy. Biospectroscopy. 4, 37–46

- Aydın, Z.Ö. (2009). Detection of Bladder Tumor Recurrence By Fourier Transform Infrared Spectroscopy As A Novel Method. Master thesis, Middle East Technical University, Ankara

- Bacon, J. S. D.; Dickinson, B. (1957). The origin of melezitose: A biochemical relationship between the lime tree (Tilia sp.) and an aphis (Eucallipterus tiliae L.).Biochemistry. 66, 289-297.

- Baroni, M. V.; Chiabrando, G. A.; Costa, C.; Wunderlin, D. A. (2002). Assessment of the floral origin of honey by SDS-page immunoblot techniques. J. Agric. Food Chem. 50, 1362-1367.

- Ben-Bassat, H.; Polliak, A.; Rosenbaum, S.M.; Naparstek, E.; Shouval, D. and Inbar, M. (1977). Fluidity of Membrane Lipids and Lateral Mobility of Concanavalin A Receptors in the Cell Surface of Normal Lymphocytes and Lymphocytes from Patients with Malignant Lymphomas and Leukemias. Cancer Res. 37(5), 1307-1312.

- Bertrand, D.; Dufour, E. (2006). La spectroscopie infrarouge et ses applications analytiques. 2nd ed. Collection Sciences et Techniques Agroalimentaires. Lavoisier, Paris p: 660.

- Bicchi, C.; Belliardo, F.; Frattini, C. (1983). Identification of the volatile components of some Piedmontese honeys. J. Apic. Res. 22, 130-136.

- Bouseta, A.; Collin, S.; Dufour, J. P. (1992). Characteristic aroma profiles of unifloral honeys obtained with a dynamic headspace GC-MS system. J. Apic. Res. 31, 96-109.

- Bouseta, A.; Scheirman, V.; Collin,S. (1996). Flavor and free amino acid composition of lavender and eucalyptus honey. J. Food Sci. 61, 683-687.

- Brown, F.M. (2000). Urine cytology: is it still the gold standard for screening. Urol Clin North Am. 27:25-37.

- Cai, S. and Singh, R. B. (2004). A Distinct Utility of the Amide III Infrared Band for Secondary Structure Estimation of Aqueous Protein Solutions Using Partial Least Squares Methods. Biochemistry. 43, 2541-2549.

- Cakmak, G.; Togan, I.; Severcan, F. (2006). Beta-estradiol induced compositional, structural and functional changes in rainbow trout liver, revealed by FT-IR spectroscopy: a comparative study with nonylphenol. Aquat Toxicol. 77(1):53-63.

- Cakmak, G.; Togan, I.; Uğuz, C.; Severcan, F. (2003) FT-IR spectroscopic analysis of rainbow trout liver exposed to nonylphenol. Applied Spectroscopy 57:835-841.

- Campbell, Meredith F.; Wein, Alan J.; Kavoussi, Louis R., eds. Campbell-Walsh Urology: Editor-in-chief, Alan J. Wein ; Editors, Louis R. Kavoussi ... [et al.]. Philadelphia : W.B. Saunders, 2007. Print.

- Castelao, J.E.; Yuan, J.M.; Skipper, P.L.; Tannenbaum, S.R. (2001). Gender- and smoking-related bladder cancer risk. J Natl Cancer Inst. 93: 538–45

- Chang, R. (1971) Basic principles of spectroscopy, McGraw Hill, New York

- Chen, M.; Irudayaraj, J. (1998). Sampling technique for cheese analysis by FTIR spectroscopy. J. Food Sci. 63, 96-99.

- Chen, R.J.; Ho, Y.S.; Guo, H.R.; Wang, Y.J. (2008). Rapid activation of Stat3 and ERK1/2 by nicotine modulates cell proliferation in human bladder cancer cells. Toxicol Sci. 104:283-93.

- Chiriboga, P.; Xie, H.; Yee, D.; Zarou, D.; and Diem, M. (1998). Infrared Spectroscopy of Human Tissue. IV. Detection of Dysplastic and Neoplastic Changes of Human Cervical Tissue via Infrared Microscopy. Cell. Mol. Biol. 44:219-229.

- Choo, L. P.; Mansfield, J. R.; Pizzi, N.; et al. (1995). Infrared spectra of human central nervous system tissue: Diagnosis of Alzheimer's disease by multivariate analyses. Biospectroscopy. 1(2), 141–148.

- Cocciardi, R.A.; Ismail, A.A.; Sedman, J. (2005). Investigation of the potential utility of single-bounce attenuated total reflectance Fourier transform infrared spectroscopy in the analysis of distilled liquors and wines. Journal of agricultural and food chemistry 53: 2803-2809

- Cohenford, M. A.; Godwin, T. A.; Cahn, F.; Bhandare, P.; Caputo, T. A.; and Rigas, B. (1997). Infrared Spectroscopy of Normal and Abnormal Cervical Smears: Evaluation by Principal Component Analysis. Gynecol. Oncol. 66:59-65

- Corbella, E.; Cozzolino, D. (2005). The use of visible and near infrared spectroscopy to classify the floral origin of honey samples produced in Uruguay. J. Near Infrared Spectrosc. 13, 63-68.

- D'Arcy, B. R.; Rintoul, G. B.; Rowland, C. Y.; Blackman, A. J. (1997). Composition of Australian honey extractives. 1. Norisoprenoids, monoterpenes, and other natural volatiles from blue gum (Eucalyptus leucoxylon) and yellow box (Eucalyptus melliodora) honeys. J. Agric. Food Chem. 45, 1834-1843.

- Davies, A. M. C.; Harris, R .G. (1982). Free amino acid analysis of honeys from England and Wales: application to the determination of the geographical origin of honeys. J.Apic.Res. 21, 168-173.

- Davies, A. M. C.; Radovic, B.; Fearn, T.; Anklam, E. A. (2002). Preliminary study on the characterisation of honey by near infrared spectroscopy. J. Near Infrared Spectrosc. 10, 121-135.

- DeMay, R. M. (1995). The Art & Science of Cytopathology (Vol. Volume 1). Chicago, Il: ASCP Press.

- Devillers, J.; Morlot, M.; Pham-Delegue, M. H.; Dore, J. C. (2004). Classification of monofloral honeys based on their quality control data. Food Chem. 86, 305-312.

- Diem, M.; Griffiths, P. R.; and Chalmers, J. M. (2008). Vibrational Spectroscopy for Medical Diagnosis. London: John Wiley & Sons, 187–202.

- Dousseau, F.; Pezolet, M. (1990). Determination of the secondary structure content of proteins in aqueous solutions from their amide I and amide II infrared bands. Comparison between classical and partial leastsquares methods, Biochemistry 29, 8771-8779.

- Dovbeshko, G.I.; Chegel, V.I.; Gridina, N.Y.; Repnytska, O.P.; Shirshov, Y.M.; Tryndiak, V.P.; Todor, I.M.; and Solyanik, G.I. (2002) Surface enhanced IR FTIR spectroscopy of biological tissues absorption of nucleic acids from tumor cells: FTIR reflectance study. Biopolymer (Biospectroscopy), 67: 470–486.

- Eckel, R.; Huo, H.; Guan, H.-W.; Hu, X.; Che, X.; and Huang, W.-D. (2001).Characteristic infrared spectroscopic patterns in the protein bands of human breast cancer tissue. Vibrational Spectroscopy 27, 165–173.

- Edwards, T.J.; Dickinson, A.J.; Natale, S.; Gosling, J.; McGrath, J.S. (2006). A prospective analysis of the diagnostic yield resulting from the attendance of 4020 patients at a protocol-driven haematuria clinic. BJU Int. 97(2):301—5.

- Ellis, D.I.; Goodacre, R. (2006). Metabolic fingerprinting in disease diagnosis: biomedical applications of infrared and Raman spectroscopy. The Analyst 131: 875-885

- Epstein, J. I.; Amin, M. B.; Reuter, V. R.; and Mostofi, F. K. (1998). The World Health Organization/International Society of Urological Pathology consensus classification of urothelial (transitional cell) neoplasms of the urinary bladder.

- Eser, S.; Yakut, C.; Özdemir, R.; et al. (2010). Cancer Incidence Rates in Turkey in 2006: A Detailed Registry Based Estimation. Asian Pacific Journal of Cancer Prevention. 11:1731-39.

- Fell, R. D. (1978). The color grading of honey. Americ. Bee J. 118, 782-789.

- Ferreres, F.; Garcia-Viguera, C.; Tomas-Lorente, F.; Tomás-Barberán, F. A. Hesperetin. (1993). A marker of the floral origin of citrus honey. J. Sci. Food Agric. 61, 121-123.

- Foster, P. L.; Eisenstadt, E.; and Miller, J. H. (1983).Base substitution mutations induced by metabolically activated aflatoxin B,. Proc. Natl. Acad. Sci. (U.S.) 80: 2695-2698

- Fujioka, N.; Morimoto, Y.; Arai, T.; and Kikuchi, M. (2004). Discrimination between normal and malignant human gastric tissues by Fourier transform infrared spectroscopy. Cancer Detection & Prevention 28, 32–36.

- Fung, M. F. K.; Senterman, M. K.; Mikhael, N. Z.; Lacelle, S.; and Wong, P. T. T. (1996). Pressure-tuning Fourier transform infrared spectroscopic study of carcinogenesis in human endometrium. Biospectroscopy 2, 155–165.

- Gilbert, J.; Shepherd, M. J.; Wallwork, M. A.; Harris, R. G. (1981). Determination of the geographical origin of honeys by multivariate analysis of gas chromatographic data on their free amino acid content. J. Apic. Res. 20, 125-135.

- Gonzales, A. P.; Burin, L.; Buera, M. D. (1999). Color changes during storage of honeys in relation to their composition and initial color. Food Res. Int. 32, 185-191.

- Goodacre, R.; Radovic, B. S.; Anklam, E. (2002). Progress toward the rapid nondestructive assessment of the floral origin of European honey using dispersive Raman spectroscopy. Appl. Spectrosc. 56, 521-527.

- Griffiths, T.R.I.; Mellon, Jk. (2000). Human papillomavirus and urological tumours: 2. Role in bladder, prostate, renal and testicular cancer. Br J Urol Int. 85: 211.

- Grossman, H.B. (1998). New methods for detection of bladder cancer. Semin Urol Oncol 16:17-22.

- Gottesman, M.M.; Pastan, I.; Ambudkar, S.V. (1996). P-glycoprotein and multidrug resistance. Curr Opin Genet Dev 6:610-17.

- Gu, J.; Liang, D.; Wang, Y.; Lu, C.; Wu, X. (2005). Effects of N-acetyl transferase 1 and 2 polymorphisms on bladder cancer risk in Caucasians. Mutat Res. 581:97–104.

- Guyot, C.; Bouseta, A.; Scheirman, V.; Collin, S. (1998). Floral origin markers of chestnut and lime tree honeys. J. Agric. Food Chem. 46, 625-633.

- Hautmann, S.; Toma, M.; Lorenzo Gomez, M.F.; et al. (2004). ImmunoCyt and the HA-HAase urine tests for the detection of bladder cancer: a sideby- side comparison. Eur Urol. 46:466–71.

- Hineno, M. (1997). Infrared spectra and normal vibrations of â-Dglucopyronose. Carbohydr. Res. 56, 219-223.

- Hoccart, X.; Turrell, G. (1995). Dynamics of urea-water complexes. Journal of Molecular Structure 349:141-144

- Hochhauser, D.; Harris, A.L. (1991). Drug resistance. Br. Med. Bull. 47:178-96.

- Hollas, JM. (2002),Basic atomic and molecular spectroscopy, The Royal Society of Chemistry, UK.

- Iglesias, M. T.; de Lorenzo, C.; Polo, M. D.; Martin-Alvarez, P. J.; Pueyo, E. (2004). Usefulness of amino acid composition to discriminate between honeydew and floral honeys. Application to honeys from a small geographic area. J. Agric. Food Chem. 52, 84-89.

- International Agency for Research on Cancer. (1994). IARC Monograph on the Evaluation of the Carcinogenic Risks to Humans, Vol. 61, Schistosomes, Liver flukes and Helicobacter pylori. International Agency for Research on Cancer: Lyon.

- Isabelle, M.; Stone, N.; Barr, H.; et al. (2008). Lymph node pathology using optical spectroscopy in cancer diagnostics. Spectroscopy: An International Journal 22 (2–3), 97–104.

- Jackson, M.; Ramjiawan, B.; Hewko, M.; and Mantsch, H. H. (1998). Infrared microscopic functional group mapping and spectral clustering analysis of hypercholosterolomic rabbit liver. Cellular and Molecular Biolog. 44(1): 89-98.

- Jamin, N.; Dumas, P.; Moncuit, J.; Fridman, W.; Teillaud, J.; Carr, L.G.; Williams, G. P. (1998). Highly resolved chemical ımaging of living cells by using synchrotron anfrared microspectroscopy. Applied Biological Sciences. 95(9): 4837-4840.

- Jemal, A.; Bray, F.; Center, M. M.; Ferlay, J.; Ward, E.; Forman, D. (2011). Global Cancer Statistics. Ca. Cancer J. Clin. 61:69–90.

- Kelly, J.G.; Trevisan, J.; Scott, A. D.; Carmichael, P.L.; Pollock, H. M.; Martin-Hirsch, P.L. and Martin, F. L. (2011). Biospectroscopy to metabolically profile biomolecular structure: a multistage approach linking computational analysis with biomarkers, J. Proteome Res. 10, 1437–1448.

- Jiang, X.; Yuan, J.M.; Skipper, P.L.; Tannenbaum, S.R.; Yu, M.C. (2007). Environmental tobacco smoke and bladder cancer risk in never smokers of Los Angeles county. Cancer Res. 67:7540-5.

- Kazarian, S. G.; Chan, K. L. (2006). Applications of ATR-FTIR spectroscopic imaging to biomedical samples. Biochim. Biophys. Acta. 1758, 858–865.

- Kerkvliet, J. D.; Meijer, H. A. J.(2000). Adulteration of honey: relation between microscopic analysis and delta C-13 measurements. Apidologie. 31, 717-726.

- Kerkvliet, J. D.; Shrestha, M.; Tuladhar, K.; Manandhar, H. (1995). Microscopic detection of adulteration of honey with cane sugar and cane sugar products. Apidologie. 26, 131-139.

- Kirkwood, K. C.; Mitchell, T. J.; Smith, D. (1960). An examination of the occurrence of honeydew in honey. Analyst. 85, 412-416.

- Kondepati, V. R.; Keese, M.; Heise, H. M.; and Backhaus J. (2006). Detection of structural disorders in pancreatic tumour DNA with Fourier-transform infrared spectroscopy. Vibrational Spectroscopy 40(1), 33–39.

- Korenius, T.; Laurikkala, J.; Juhola, M. (2007). On principal component analysis, cosine and Euclidean measures in information retrieval. Inform. Sci. 177, 4893–4905.

- Krauze, A.; Zalewski, R. I. (1991). Classification of honeys by principal component analysis on the basis of chemical and physical parameters. Z. Lebensm. Unters.Forsch. 192, 19-23.

- Levin, I. W.; Bhargava, R. (2005). Fourier transform infrared vibrational spectroscopic imaging: Integrating Microscopy and Molecular Recognition. Annu. Rev. Phys. Chem. 56, 429–474.

- Li, Q.B.; Sun, X.J.; Xu, Y.Z.; et al. (2005). Diagnosis of gastric inflammation and malignancy in endoscopic biopsies based on Fourier transform infrared spectroscopy. Clinical Chemistry 51(2), 346–350

- Lichtenberg-Kraag, B.; Hedtke, C.; Bienefeld, K. (2002). Infrared spectroscopy in routine quality analysis of honey. Apidologie. 33, 327-337.

- Liu, C.; Zhang, Y.; Yan, X.; Zhang, X.; Li, C.; Yang, W.; Shi, D. (2006). Infrared absorption of human breast tissues in vitro. Journal of Luminescence. 119–120 (2006) 132–136.

- Louveaux, J.; Maurizio, A.; Vorwohl, G. (1978). Methods of melissopalynology. Bee World. 59, 139-162.

- Lucassen, G. W.; Van Veen, G. N.; and Jansen, J. A. (1998). Band analysis of hydrated human skin stratum corneum attenuated total reflectance Fourier transform infrared spectra in vivo. J. Biomed. Opt. 3, 267–280.

- Lum, B.L.; Gosland, M.P.; Kaubisch, S.; Sikic, B.I. (1993). Molecular targets in oncology: implications of the multidrug resistance gene. Pharmacotherapy. 13:88-109.

- Manikis, I.; Thrasyvoulou, A. (2001). The relation of physico-chemical characteristics of honey and the crystallization sensitive parameters. Apiacta. 36, 106-112.

- Mansfield, C.; Man, A.; Low-Ying, S.; Shaw, RA. (2005). Laminar Fluid Diffusion Interface Preconditioning of Serum and Urine for Reagent-Free Infrared Clinical Analysis and Diagnostics. Applied Spectroscopy. 59(1): 10-15.

- Manoharan, R.; Baraga, J. J.; Rava, R. P.; Dasari, R. R.; Fitzmaurice, M. and Feld, M. S. (1993) Biochemical analysis and mapping of atherosclerotic human artery using FTIR microspectroscopy. Atherosclerosis. 103:181-193.

- Mantsch, H.H. (1984). Biological application of Fourier Transform Infrared Spectroscopy: A study of phase transitions in biomembranes. J. Mol. Structure. 113: 201-212.

- Marcelli, A.; Cricenti, A.; Kwiatek, W.M.; Petibois, C. (2012). Biological applications of synchrotron radiation infrared spectromicroscopy. Biotechnology advances. 30(6):1390-404.

- Martin, F. L.; Pollock, H. M. (2010). In Oxford Handbook of Nanoscience and Technology; Narlikar, A. V., Fu, Y. Y., Eds.; Oxford University Press: UK, Vol. 2, Chapter 8, pp 285-336.

- Mateo, R.; Bosch-Reig, F. (1998). Classification of Spanish unifloral honeys by discriminant analysis of electrical conductivity, color, water content, sugars, and pH. J.Agric. Food Chem. 46, 393-400.

- Mateo, R.; Bosch-Reig, F. (1997). Sugar profiles of Spanish unifloral honeys. Food Chem. 60, 33-41.

- Mato, I.; Huidobro, J. F.; Sanchez, M. P.; Muniategui, S.; Fernández-Muiño, M. A.; Sancho, M. T. (1997). Enzymatic determination of total D-gluconic acid in honey. J. Agric. Food Chem. 45, 3550-3553.

- Maziak, D. E.; Do, M. T.; Shamji, F. M.; Sundaresan, S. R.; Perkins, D. G. and Wong, P. T. T. (2007). Fourier-transform infrared spectroscopic study of characteristic molecular structure in cancer cells of esophagus: An exploratory study. Cancer and Prevention. 31(3), 244–253.

- McIntosh, I. M.; Jackson, M.; Mantsch, H. H. et al. (1999). Infrared spectra of basal cell carcinomas are distinct from non-tumour-bearing skin components. J. Invest. Dermatol. 112, 951–956.

- Melin, A.; Perromat, A. and Deleris, G. (2000). Pharmacologic application of Fourier transform IR spectroscopy: In vivo toxicity of carbon tetrachloride on rat liver. Biopolymers (Biospectroscopy). 57:160-168.

- Melin, A.M.; Perromat, A. and Deleris, G. (2001). Fourier-transform infrared spectroscopy: a pharmacotoxicologic tool for in vivo monitoring radical aggression. Canadian Journal of Physiology and Pharmacology. 79 (2):158-165.

- Messing, E.M.; Young, T.B.; Hunt, V.B. (1995). Comparision of bladder cancer outcome in men undergoing hematuri home screening versus those with standard clinical presentation. Urology. 45: 487.

- Mordechai, S.; Mordechai, J.; Ramesh, J.; Levi, C.; Huleihel, M.; Erukhimovitch, V.; Moser, A. and Kapelushnik, J. (2001). Application of FTIR microspectroscopy for the follow-up of childhood leukaemia chemotherapy. Proc. SPIE Subsurface and Surface Sensing Technologies and Applications III. 4491, 243–250.

- Nakazawa, I.; Iwaizumi, M. (1989). A Role of the Cancer Cell Membrane Fluidity in the Cancer Metastases: An ESR Study. Tohoku J. Exp. Med. 157: 193-198.

- Nasuhoğlu, R.; Tokmakçıoğlu, E. (1969). Modern Üniversite Fiziği, Ankara Üniversitesi, 169, Ankara.

- Naumann, D.; Helm, D.; Labischinski, H. (1991). Microbiological characterizations by FT-IR Spectroscopy. Nature. 351, 81-82.

- Ouerhani, Rouissi, K.; Kourda, N.; Marrakchi, R.; Bougatef, K.; Riadh Ben Slama, M.; Sfaxi, et al. (2009). Combined analysis of smoking, TP53, and FGFR3 mutations in Tunisian patients with invasive and superficial high-grade bladder tumors. Cancer Invest. 27:998-1007.

- Paradkar, M. M.; Irudayaraj, J. (2002). Discrimination and classification of beet and cane inverts in honey by FT-Raman spectroscopy. Food Chem. 76, 231-239.

- Perez, R. A.; Sanchez-Brunette, C.; Calvo, R. M.; Tadeo, J. L. (2002). Analysis of volatiles from Spanish honeys by solid-phase microextraction and gas chromatography-mass spectrometry. J. Agric. Food Chem. 50, 2633-2637.

- Perkins, W. D. (1987). Fourier Transform Infrared Spectroscopy, Part II. Advantages of FT-IR. J, Chem. Educ. 64.

- Persano Oddo, L.; Piro, R. (2004). Main European unifloral honeys: descriptive sheets.Apidologie. 35 (special issue), 38-81.

- Pfister, C.; Chautard, D.; Devonec, M., et al. (2003). ImmunoCyt test improves the diagnostic accuracy of urinary cytology: results of a French multicenter study. J Urol. 169:921–4.

- Piana, L.; Persano Oddo, L.; Bentabol, A.; Bruneau, E.; Bogdanov, S.; Guyot-Declerck, C.(2004). Sensory analysis applied to honey: state of the art. Apidologie. 35 (special issue), 26-37.

- Piazza, M. G.; Accorti, M.; Persano Oddo, L. (1991). Electrical conductivity, ash, colour and specific rotatory power in Italian unifloral honeys. Apicoltura. 51-63.

- Piro, R.; Guidetti, G.; Persano Oddo, L.; Piazza, M. G. (2002). Mathematical diagnosis of unifloral honeys. In Il ruolo della ricerca in apicoltura; Sabatini, A. G.; Bolchi- Serrini, G.; Frilli, R.; Porrini, C., Eds.; Litosei: Bologna.

- Prout, G.R.; Barton, B.A.; Griffin, P.P.; Friedell, G. (1992). Treated history of noninvasive grade 1transitional cell carcinoma. J Urol. 148: 1413.

- Radovic, B. S.; White, R.; Parker, I.; Dennis, M. J.; Sharman, M.; Geiss, H.; Anklam, E. (2001). Contribution of high temperature gas chromatographic analysis of oligosaccharides and ion chromatographic analysis of various cations and anions to authenticity testing of honey. Dtsch. Lebensm. Rundschau. 97, 380-384.

- Ramakumar, S.; Bhuiyan, J.; Besse, J.A.; Roberts, S.G.; Wollan, P.C.; Blute, M.L., et al. (1999). Comparison of screening methods in the detection of bladder cancer. J Urol. 161:388-94.

- Reuter, V. E.; Epstein, J. I.; Amin, M. B. and Mostofi, F. K. (1999). Bladder Consensus Conference Committee. Am J Surg Pathol. 22(12), 1435-1448.

- Rigas, B.; Morgello, S.; Goldman, I. S. and Wong, P. T. T. (1990). Human colorectal cancers display abnormal Fourier transform infrared spectra. Proc. Natl. Aca. Sci. USA. 87:8140-8144.

- Rowland, C. Y.; Blackman, A. J.; D'Arcy, B. R.; Rintoul, G. B. (1995). Comparison of organic extractives found in leatherwood (Eucryphia lucida) honey and leatherwood flowers and leaves. J. Agric. Food Chem. 43, 753-763.

- Ruoff, K. (2006). Authentication of the Botanical origion of honey. Doctoral dissertation, Swiss Fedaral Institute of Technology, Zurich.

- Russmann, H. (1998). Hefen und Glycerin in Blütenhonigen - Nachweis einer Gärung oder einer abgestoppten Gärung. Lebensmittelchemie. 52, 116-117.

- Sabatini, A. G.; Persano Oddo, L.; Piazza, M. G.; Accorti, M.; Marcazzan, G. (1990). Glucide spectrum in the main Italian unifloral honeys. II. Di- and trisaccharides. Apicoltura. 6, 63-70.

- Sanz, M.L.; Gonzalez, M.; de Lorenzo,C.; Sanz,J.; Martinez-Castro,I. A. (2005). Contribution to the differentiation between nectar honey and honeydew honey. Food Chem. 91, 313-317.

- Severcan, F.; Gorgulu, G.; Turker Gorgulu S.; Guray T. (2005). Rapid monitoring of diabetes-induced lipid peroxidation by Fourier transform infrared spectroscopy: Evidence from rat liver microsomal membranes. Anal. Biochem. 339:36–40.

- Severcan, F.; Toyran, N.; Kaptan, N. and Turan, B. (2000). Fourier transform infrared study of diabetes on rat liver and heart tissues in the C-H region. Talanta. 53: 55-59.

- Severcan, F. and Haris, P. I. (1999). FTIR spectroscopic characterization of protein structure in aqueous and non-aqueous media. Journal of Molecular Catalysis B. Enzymatic. 7: 207-221.

- Severcan, F. (1997). Vitamin E Decreases the Order of the Phospholipid Model Membranes in the Gel Phase: An FTIR Study. Bioscience Reports. 7 (2): 231-235

- Siede, R.; Schmidt, C.; Büchler, R. (2004). A PCR based apple detection method as a complementary instrument for the honey quality assessment. Dtsch. Lebensm. Rundschau. 100, 381-384.

- Sindhuphak, R.; Issaravanich, S.; Udomprasertgul, V., et al. (2003). A new approach fort he detection of cervical cancer in Thai woman.Gynocologic Oncology. 90, 10-14.

- Skoog D.A.; Holler F.J.; Nieman T.A. (1984) Principles of Instrumental Analysis, Harcourt College Publishers

- Soloway, M.S., Bruck, D.S., Kim, S.S. (2003). Expectant management of small, recurrent, noninvasive papillary bladder tumors. J Urol. 170:438–41.

- Soria, A. C.; Gonzalez, M.; de Lorenzo, C.; Martinez-Castro, I.; Sanz, J. (2004). Characterization of artisanal honeys from Madrid (Central Spain) on the basis of their melissopalynological, physicochemical and volatile composition data. Food Chem. 85, 121-130.

- Steinbeck, G.; Plato, N.; Norell, S.E. (1990). Urothelial cancer and some industry-related chemicals: An evaluation of the epidemiologic literature. Am. J. Ind. Med. 17:371.

- Stuart, B. (2004). Infrared Spectroscopy: Fundamentals and Applications. John Wiley and Sons, Ltd., England.

- Takahashi, H.; French, S. M.; and Wong, P. T. T. (1991). Alterations in hepatic lipids and proteins by Chronic ethanol Intake: A highpressure fourier transform Infrared spectroscopic study on alcoholic liver disease in the rat alcohol. Clin. Exp. Res. 15(2): 219-223.

- Tantipolphan R.; Rades T.; and Medlicott N.J. (2008). Insights into the Structure of Protein by Vibrational Spectroscopy. Current Pharmaceutical Analysis. 4; 53–68.

- Tewari, J. C.; Irudayaraj, J. M. K. (2005). Floral classification of honey using mid-infrared spectroscopy and surface acoustic wave based z-Nose sensor. J. Agric. Food Chem. 53, 6955-6966.

- Tewari, J.; Irudayaraj, J. (2004). Quantification of saccharides in multiple floral honeys using Fourier transform infrared micro-attenuated total reflectance spectroscopy. J. Agric. Food Chem. 52, 3237-3243.

- Toyran, N.; Lasch, P.; Naumann, D.; Turan, B. and Severcan F. (2006). Early alterations in myocardia and vessels of the diabetic rat heart:an FTIR microspectroscopic study. Biochem. J. 397, 427–436.

- Tul'chinsky, V. M.; Zurabian, S. F.; Asankozhoev, K. A.; Kogan, G. A.; Khorlin, A. Y. (1976). Study of infrared spectra of oligosaccharides in the region 1000-400 cm^{-1}. Carbohydr. Res. 51,1-15.

- Von der Ohe, W.; Persano Oddo, L.; Piana, M. L.; Morlot, M.; Martin, P. (2004). Harmonized methods of melissopalynology. Apidologie, 35, (special issue), 18-25.

- Vriesema, J.L.; Atsma, F.; Kiemeney, L.A.; Peelen, W.P.; Witjes, J.A.; Schalken, J.A. (2001). Diagnostic efficacy of the ImmunoCyt test to detect superficial bladder cancer recurrence. Urology. 58:367– 71.

- Wang, H. P.; Wang, H.-C.; and Huang, Y.-J. (1997). Microscopic FTIR studies of lung cancer cells in pleural fluid. The Sci. Total Envir. 204, 283–287.

- Weston, R. J.; Brocklebank, L. K.; Lu, Y. (2000). Identification of quantitative levels of antibacterial components of some New Zealand honey. Food Chem. 70, 427-435.

- Wojciechowski, C.; Dupu, N.; Ta, C. D.; Huvenneb, O J. P. and Legrand, P. (1998). Quantitative analysis of water-soluble vitamins by ATR-FTIR spectroscopy. Food Chem. 63(1), 133-140.

- Wong, P.T.T.; Goldstein, S.M.; Grekin, R.; Godwin, T.A.; Pivik, C.; Rigas, B. (1993). Distinct Infrared Spectroscopic Patterns of Human Basal Cell Carcinoma of the Skin. Cancer Research. 53, 762-765.

- Wong, P. T. T. (1987). Vibrational spectroscopy under high pressure In: J. R. Durig (ed.) Vibrational Spectra and Structure, Vol. 16, pp. 357-445. Amsterdam: Elsevier.

- Wong, P. T. T;, and Rigas, B. (1990). Infrared spectra of microtome sections of human colon tissues. Appl. Spectrosc., 44: 1715-1718.

- Wong, P. T. T., Mantsch, H. (1988). Reorientational and conformational ordering processes at elevated pressure in 1,2-dioleyl phosphatidyl choline. Biophys. J., 54:781-790.

- Wong, P. T. T.; Wong, R. K.; Caputo, T. A; Godwin T. A.; Rigas B. (1991). Infrared Spectroscopy of Exfoliated Human Cervical Cells: Evidence of Extensive Structural Changes During Carcinogenesis. Proc. Natl. Acad. Sci. 88, 10988-10992.

- Wood, B. R.; Quinn, M. A.; Burden, F. R.; and McNaughton, D. (1996). An investigation into FT-IR spectroscopy as a bio-diagnostic tool for cervical cancer. Biospectroscopy. 2, 143–153.

- Wu, X.; Ye, Y.; Kiemeney, L.A.; et al. (2009). A multi-stage genome-wide association study of bladder cancer identifies multiple susceptibility loci. Nat Genet. 41:991–5.

- Xu, Y. Z.; Yang, L. M.; Xu, Z.; et al. (2005). Distinguishing malignant from normal stomach tissues and its in vivo, in situ measurement in operating process using FTIR Fibre-Optic techniques. Science in China Series B-Chemistry. 48(2), 167–175.

- Yang, Y.; Sule-Suso, J.; Sockalingum, G. D.; Kegelaer, G.; Manfait, M.; and El Haj, A. J. (2005). Study of tumour cell invasion by Fourier transform infrared microspectroscopy. Biopolymers. 78, 311–317.

- Yano, K.; Ohoshima, S.; Grotou, Y.; Kumaido, K.; Moriguchi, T.; and Katayama, H. (2000). Direct measurement of human lung cancerous and noncancerous tissues by Fourier transform infrared microscopy: Can an infrared microscope be used as a clinical tool. Analytical Biochemistry. 287, 218–225.

- Zeisig, R.; Koklic, T.; Wiesner, B.; Fichtner, I.; Sentjurc, M. (2007). Increase in fluidity in the membrane of MT3 breast cancer cells correlates with enhanced cell adhesion in vitro and increased lung metastasis in NOD/SCID mice. Archives of Biochemistry and Biophysics. 459 98–106.

- Zirong, Q.; Ling, S.; Jinwei, L. (1991). Dynamic parameter of membrane lipid in lung cancer cell lines, carcinogenesis cells and cancer cells isolated from patients with lung cancer. Chinese Journal of Cancer Research. 3(4): 24-30.